

Dynamical learning of dynamics

Christian Klos,¹ Yaroslav Felipe Kalle Kossio,¹ Sven Goedeke,¹ Aditya Gilra,^{1,2} and Raoul-Martin Memmesheimer¹

¹*Neural Network Dynamics and Computation, Institute of Genetics, University of Bonn, Bonn, Germany.*

²*Department of Computer Science, and Neuroscience Institute, University of Sheffield, Sheffield, UK.*

The ability of humans and animals to quickly adapt to novel tasks is difficult to reconcile with the standard paradigm of learning by slow synaptic weight modification. Here we show that fixed-weight neural networks can learn to generate required dynamics by imitation. After appropriate weight pretraining, the networks quickly and dynamically adapt to learn new tasks and thereafter continue to achieve them without further teacher feedback. We explain this ability and illustrate it with a variety of target dynamics, ranging from oscillatory trajectories to driven and chaotic dynamical systems.

Introduction. Humans and animals can learn wide varieties of tasks. The predominant paradigm assumes that their neural networks achieve this by slow adaptation of connection weights between neurons [1, 2]. Neurobiological experiments, however, also indicate fast learning with static weights [3]. Our study addresses how neural networks may quickly learn to generate required output dynamics without weight-learning.

The goal of neural network learning is ultimately to appropriately change the activity of the output neurons of the network. In supervised learning, it should match a target and continue doing so during subsequent testing; in reinforcement learning, it should maximize a sparsely given reward. In our study, the networks adapt their weights during a pretraining phase [4–6] such that thereafter with static weights they achieve supervised learning of desired outputs, by adapting only their dynamics (dynamical learning). Adapting the static network’s weights during pretraining is thus a kind of meta-learning or learning-to-learn. There is a recent spurt of interest in learning-to-learn [5, 6], focusing mainly on learning of reinforcement learning [7–9]. Studies on learning of supervised dynamical learning showed prediction of a time series at the current time step given the preceding step’s target [10–19] and control of a system along a time-varying target [20–23]. The studies assume that a target is present during testing to avoid unlearning. This limits applicability and renders the dynamics necessarily non-autonomous; it is conceptually problematic for supervised settings and at odds with the common concept of teacher-free recall.

We therefore develop a scheme for fast supervised dynamical learning and subsequent teacher-free generation of long-term dynamics. We consider models for biological recurrent (reciprocally connected) neural networks, where leaky rate neurons interact in continuous time [1, 2]. Such models are amenable to learning, computation and phase space analysis [1, 2, 24–26]. After appropriate pretraining using the reservoir computing scheme (where only the weights to output neurons are trained [25, 27, 66, 67]), all weights are fixed. The networks can nevertheless learn to generate new, desired dynam-

ics. Furthermore, they continue to generate them in self-contained manner during subsequent testing. We illustrate this with a variety of trajectories and dynamical systems and analyze the underlying mechanisms.

Network model. We use recurrent neural networks, where each neuron (or neuronal subpopulation) i , $i = 1, \dots, N$, with N between 500 and 3000 depending on the task [27], is characterized by an activation variable $x_i(t)$ and communicates with other neurons via its firing rate $r_i(t)$, a nonlinear function of $x_i(t)$ [1, 2]. In isolation $x_i(t)$ decays to zero with a time constant τ_i . This combines the decay times of membrane potential and synaptic currents. The network has two outputs, which can be interpreted as linear neurons: signal $z_k(t)$, $k = 1, \dots, N_z$, and context $c_l(t)$, $l = 1, \dots, N_c$ (Fig. 1). After learning, $z(t)$ generates the desired dynamics while $c(t)$ indexes it. They are continually fed back to the network, allowing their autonomous generation [66]. The networks are temporarily also informed about their signal’s difference from its target $\tilde{z}(t)$ by an error input $\varepsilon(t) = z(t) - \tilde{z}(t)$. Taken together, for constant weights the network dynamics are given by

$$\begin{aligned} \tau \dot{x}(t) &= -x(t) + Ar(t) + w_z z(t) + w_c c(t) \\ &\quad + w_\varepsilon \varepsilon(t) + w_u u(t), \\ z(t) &= o_z r(t), \quad c(t) = o_c r(t), \end{aligned} \quad (1)$$

with recurrent weights A , the diagonal matrix of time constants τ , signal and context output weights o_z , o_c , feedback weights w_z , w_c , input weights w_ε , w_u and a drive $u(t)$ absent for most tasks. We choose $r_i(t) = \tanh(x_i(t) + b_i)$ [25, 66, 68]; offsets b_i are drawn from a uniform distribution between -0.2 and 0.2 and break the $x \rightarrow -x$ symmetry without input. Unless mentioned otherwise, we set $\tau_i = 1$ fixing the overall time scale. Recurrent weights A_{ij} are set to zero with probability $1 - p$ ($p = 0.1$ or $p = 0.2$ depending on the task). Nonzero weights are drawn from a Gaussian distribution with mean 0 and variance $\frac{g^2}{pN}$, where $g = 1.5$ [25]. $w_{z,ij}$, $w_{c,ij}$ and $w_{\varepsilon,ij}$, $w_{u,ij}$ are drawn from a uniform distribution between $-\tilde{w}$ and \tilde{w} ($\tilde{w} = 1$ or $\tilde{w} = 2$).

Pretraining. The aim of our pretraining (Fig. 1a) is twofold. First, it should enable the resulting static networks to learn signals of a specific class given only the

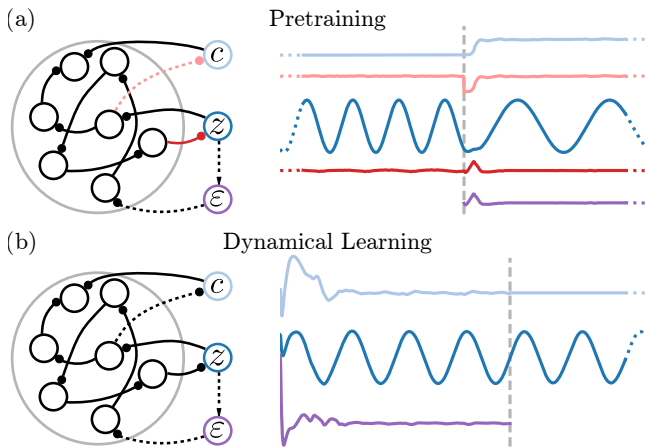


FIG. 1. Pretraining and learning. (a) During pretraining, the output weights (left, different reds) of the network are adapted using the output errors $\varepsilon(t) = z(t) - \tilde{z}(t)$ (right, red) and $c(t) - \bar{c}(t)$ (light red), such that $z(t)$ (blue, different scale for clarity) and $c(t)$ (light blue) match their targets. Different members of the target family are weight-learned in the training periods (dashed vertical). At their beginnings, $\varepsilon(t)$ is fed also as input (purple). (b) Dynamical learning. The output weights are now fixed. The network receives the signal error $\varepsilon(t)$ as input (purple). It adapts its dynamics to generate $z(t) \approx \tilde{z}(t)$ (blue). During testing, an error is no longer provided and $c(t)$ is fixed to its previous average (right, dashed vertical, left, dashed weights). $z(t)$ continues to approximate $\tilde{z}(t)$.

error input $\varepsilon(t)$. Second, after removing the error input the static networks should be able to continue to generate the desired dynamics. Therefore, the networks have to learn to minimize $\varepsilon(t)$ and, as explained in the Analysis section, to associate unique contexts with the different target dynamics.

To achieve this, we present different trajectories $\tilde{z}(t)$ of the target class to the networks, together with associated, straightforwardly chosen constant indices \bar{c} . The output weights $o_{z,ij}$ and $o_{c,ij}$ learn online according to the FORCE rule [25, 27] to minimize the output errors $\varepsilon(t)$ and $c(t) - \bar{c}$. In short, they are modified using the supervised recursive least-squares algorithm with high learning rate. This provides a least-squares optimal regularized solution for the output weights given the past network states and targets [69]. Signals and indices are presented for a time t_{wlearn} (30000 or 50000) as a continuous, randomly repeating sequence of training periods of duration t_{stay} (between 200 and 1000). During each training period's first part, a network receives $\varepsilon(t)$ as input. Because of the various last states of the previous learning periods, it thus learns to approach $\tilde{z}(t)$ from a broad range of initial conditions given this input. In most of our tasks, after a time $t_{\text{fb}} = 100$, when $z(t)$ is close to $\tilde{z}(t)$, $\varepsilon(t)$ is switched off and $c(t)$ is fixed to its constant target, matching the testing paradigm. This often helps the network to learn generation of $z(t) \approx \tilde{z}(t)$ without

error input.

Dynamical learning and testing. The weights now remain static and the error input teaches the network new tasks of the pretrained target class (Fig. 1b), i.e. the networks dynamically learn to generate $z(t) \approx \tilde{z}(t)$ for previously unseen $\tilde{z}(t)$. The learning time t_{learn} (between 50 and 200) is short, a few characteristic timescales of the target dynamics [27]. $c(t)$ is moderately fluctuating.

Thereafter the test phase begins, where no more teacher is present ($w_\varepsilon \rightarrow 0$). In weight-learning paradigms, during such phases the weights are fixed [25, 66, 67, 70, 71]. We likewise fix $c(t)$ to a temporally constant value, an average of previously assumed ones, $c(t) = \bar{c}$. This may be interpreted as indicating that the context is unchanged and the same signal is still desired. We find in our applications, that the network dynamics continue to generate a close-to-desired signal $z(t)$, establishing the successful dynamical learning of the task.

Applications. We illustrate our approach by learning a variety of trajectories (tasks (i-iv)) and dynamical systems (tasks (v,vi)). First, we consider a family $\tilde{z}(t; k)$ of target trajectories, parameterized by k . The networks are pretrained on a few of them, where the context target \bar{c} is a linear function of k . Thereafter the networks dynamically learn to generate a previously unseen trajectory as output and perpetuate it during testing. We start with the simple, instructive target family of oscillations with different periods (task (i)): $\tilde{z}(t; T) = 5 \sin(\frac{2\pi}{T}t)$. We use three different teacher trajectories for pretraining, with $T = 10, 15, 20$. After pretraining, our networks can precisely dynamically learn oscillations with unseen periods within and slightly beyond the pretrained ones (Fig. 2a,b, see [27] for further detail and analysis of learning performance of all tasks). Next, in (ii), we generalize (i) to higher order Fourier series. Specifically, we consider the target family of superpositions of two random Fourier series with weighting factor λ : $\tilde{z}(t; \lambda) = (1 - \lambda)\tilde{z}_1(t; \lambda) + \lambda\tilde{z}_2(t; \lambda)$. Here, $\tilde{z}_l(t; \lambda)$, $l = 1, 2$, are Fourier series of order O and period $T(\lambda) = (1 - \lambda)T_1 + \lambda T_2$. T_l and the Fourier coefficients are drawn randomly. We use seven different teacher trajectories for pretraining, with weighting factors distributed equidistantly between 0 and 1. After pretraining, we test the dynamical learning for thirteen weighting factors also distributed equidistantly between 0 and 1. To quantify the learning performance, we determine the fraction of these targets that can be successfully learned (RMSE below given threshold (0.4) and below RMSE between signal and (other) pretrained targets). We find that networks of increasing size can learn Fourier series with increasing order (Fig. 2c,d). Networks with 3000 neurons learn Fourier series of order 10 with a median fraction of successes of close to 90%. Hence, very general periodic functions can be learned. The highest producible frequency is limited by the available neuronal time scales τ_i . We thus expect that larger networks containing smaller

τ_i can learn even higher order targets.

To check if our approach also works for a target family with more than one parameter and multidimensional trajectories, we consider in (iii) a superposition of sines with different amplitude and period (consequently k, \tilde{c} are two-dimensional vectors) and in (iv) a set of fixed points along a curve in three-dimensional space. We find that, after pretraining, our networks are able to dynamically learn unseen members of these target families with multidimensional context or signal, as shown in Fig. 3a,b for example trajectories.

Second, we consider a family $\dot{\tilde{z}}(t) = F(\tilde{z}(t), u(t); k)$ of target dynamical systems. The networks are pretrained on a few representative systems. Thereafter, an unseen one is dynamically learned. Learning is in both phases based on imitation of trajectories. However, in contrast to tasks (i-iv) the networks now need to generate unseen output trajectories during testing. To demonstrate dynamical learning of a driven system, we consider task (v) of approximating the trajectory of an overdamped pendulum with drive $u(t)$ and different masses m : $\dot{\tilde{z}}(t) = F(\tilde{z}(t), u(t); m)$. During pretraining and dynamical learning, we use low-pass filtered white noise as drive (Fig. 3c, left of dashed vertical). During testing, we use a triangular wave (Fig. 3c, right of dashed vertical). As our networks nevertheless generate the correct qualitatively different signal (Fig. 3c,d), they must have learned the underlying vector field $F(\tilde{z}, u; m)$. (v) also shows that learning goes beyond interpolation of trajectories (compare blue and gray traces in Fig. 3d). Finally, in task (vi) we show dynamical learning of chaotic dynamics, considering autonomous Lorenz systems with different dissipation parameter β of the z -variable. For chaotic dynamics, even trajectories of similar systems quickly diverge. The aim in this task is thus only to generate during testing signals of the same type as the trajectories of the target system. We test this by comparing the limit sets of the dynamics and the tent-map relation between subsequent maxima of the z -coordinate (Fig. 3e,f). The reproduction of the tent-map relation further shows that our approach can generate not explicitly trained quantitative dynamical features. We note that the networks also dynamically learn the fixed point convergence of some of the targets in the considered parameter space, even though they were pretrained on chaotic dynamics only [27].

Analysis. In the following we analyze the different parts of our network learning and its applicability. One interpretation of the pretraining phase is that the network learns a negative feedback loop, which reduces the error $\varepsilon(t)$. For another interpretation, we split $\varepsilon(t)$ and regroup the z -dependent part of Eq. (1) as $(w_z + w_\varepsilon)z(t) - w_\varepsilon\tilde{z}(t)$: feeding back $\varepsilon(t)$ is equivalent to adding a teacher drive $\tilde{z}(t)$, except for a specific change in the feedback weights w_z . For the z -output alone the network thus weight-learns an autoencoder $\tilde{z}(t) \rightarrow z(t)$.

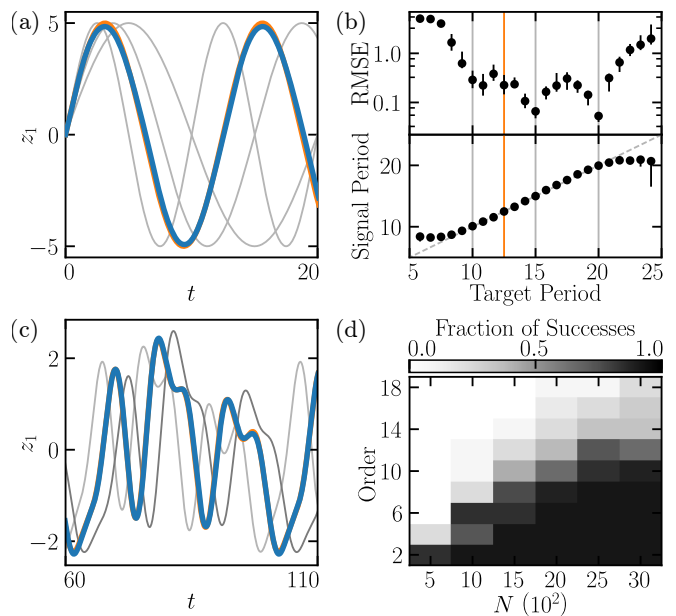


FIG. 2. Dynamical learning of periodic trajectories. (a,b) Testing after dynamical learning of sinusoids. (a) Signal (blue) matches the example testing target (orange, mostly covered by signal) well. Pretraining targets (gray traces) are clearly distinct. (b) For many different targets the root-mean-square error (RMSE) between signal and target is low (top) and the signal's period tracks the target's period well (bottom). Gray and orange verticals indicate periods of pretrained targets and target in (a). Dots show median value and errorbars interquartile range, using 10 network instances. (c,d) Testing after dynamical learning of Fourier series. (c) Like (a), for a random Fourier series with $O = 6$. Only the two closest pretrained dynamics are displayed for clarity. (d) Learning success for different network sizes and orders of the Fourier series. Color encodes median fraction of success, using 40 network instances and random Fourier series.

This is usually an easy task for reservoir networks [72]. To simultaneously learn the constant output $c(t) = \tilde{c}$, the network has to choose an appropriate o_c orthogonal to the subspaces in which the different $z(t)$ -driving r -dynamics take place. Orthogonal directions are available in sufficiently large networks, since the subspaces are low-dimensional [73].

After the correct z -dynamics are assumed, we have $\varepsilon(t) \approx 0$. Since remaining fluctuations in $\varepsilon(t)$ could stabilize the dynamics, we usually include ensuing learning phases with $w_\varepsilon \rightarrow 0$ and $c(t) = \tilde{c}$. These teach the network to generate the correct dynamics in stable manner under conditions similar to testing.

To analyze the principles underlying dynamical learning and testing, we consider task (i). The similarity of the network and learning setups suggests that the same principles underlie all our tasks. We additionally confirm this for (vi) [27]. Viewing the network dynamics in the space of firing rates r , we choose new coordinates with first axis along o_c and the principal components of the

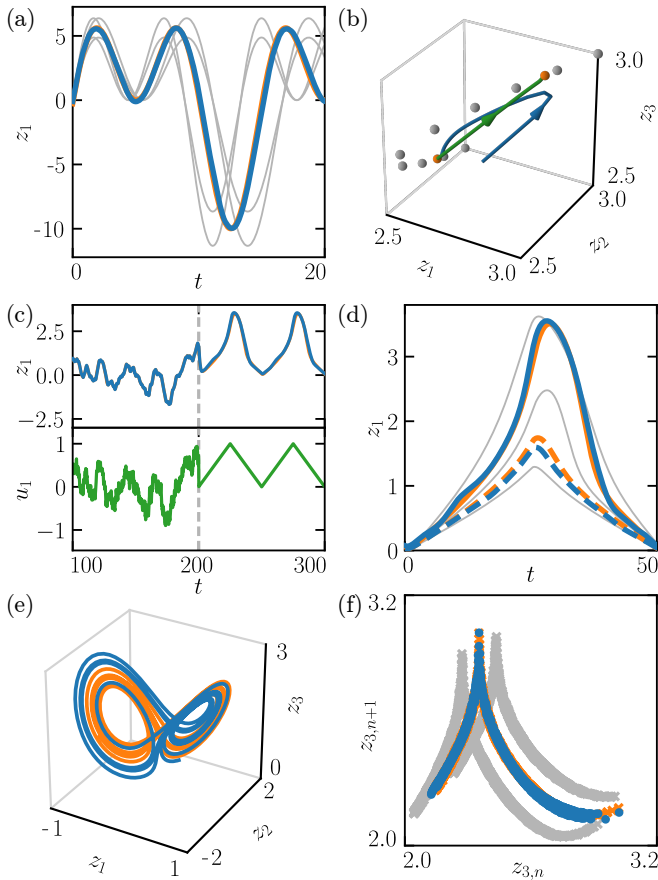


FIG. 3. Dynamical learning of different tasks. Testing phase after dynamical learning of an example (a) two-parametric superposition of sines, (b) fixed point, (c,d) driven overdamped pendulum, and (e,f) Lorenz system. (a-d) Signals (blue) match testing targets (orange, mostly covered by signal) well. Pretraining targets (gray traces or spheres) are clearly distinct. (a) displays only the four closest pretrained dynamics for clarity. (b) Signal transients (blue, green) of subsequent dynamical learning of two targets (orange spheres). (c) Signal, target and drive (green) during dynamical learning and subsequent testing (dashed vertical). (d) Dynamically learned approximations of two different pendulums (continuous, dashed), driven by the same triangular input. (e) Limit sets of signal (blue) and target (orange). (f) Tent maps of signal (blue) and dynamical (orange) and pretrained targets (gray).

dynamics orthogonal to o_c . The dynamics are then given by $c(t) = o_c r(t), r_{PC1}(t), r_{PC2}(t), \dots$ (Fig. 4). We focus on the first three coordinates, which describe large parts of the dynamics and output generation. We find that during dynamical learning, the error feedback drives the dynamics towards an orbit that is shifted in c but similar to pretrained ones. The network therewith generalizes the pretrained reaching and generation of orbits together with corresponding, near-constant $c(t)$, while $\varepsilon(t)$ is fed in. We note that the combination of current state and error input is important (see Fig. 4a for $w_\varepsilon \rightarrow 0$ and a

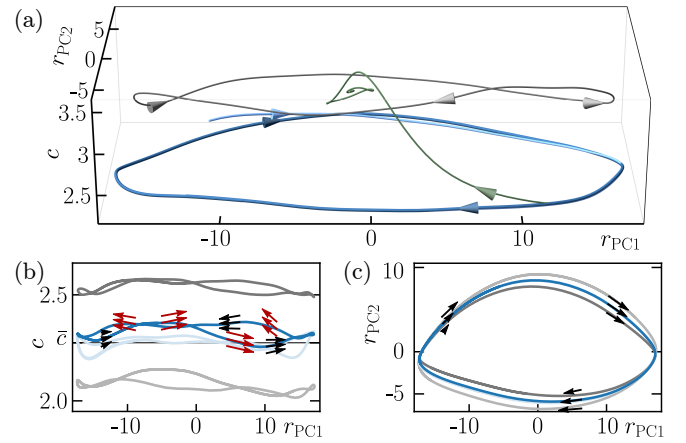


FIG. 4. Network dynamics during dynamical learning (a) and testing (b,c) of task (i), in c, r_{PC1}, r_{PC2} -coordinates. (a) During dynamical learning, the error input drives the network to a periodic orbit (light blue trajectory) and keeps it there (blue). Without input, the dynamics converge to a stable orbit (gray) whose signal approximates a pretrained one. Freezing $\tilde{z}(t) = \tilde{z}(t_0)$ drives the dynamics to a fixed point off the orbit (green). (b) During testing, the assumed orbit (blue) in the c - r_{PC1} -plane is similar to the error driven one (light blue, closest pretrained orbits with $c(t)$ fixed to their \tilde{c} : gray). The constant feedback \tilde{c} prevents the dynamics to leave the region where $c(t) \approx \tilde{c}$, compare $\dot{r}(r)$ (black vectors, r on/nearby trajectory) with $\dot{r}(r)$ for variable feedback $c(t)$ (red vectors). (c) All four orbits are similar in the r_{PC1} - r_{PC2} -plane. The dynamically learned orbit has an attracting projected vector field (black vectors) like the pretrained orbits.

mismatched $\tilde{z}(t) = \tilde{z}(t_0)$ for $t > t_0$).

During testing, the network generalizes the pretrained characteristics that feeding back $w_c \tilde{c}$ leads to $c(t) \approx \tilde{c}$. Clamping $w_c c(t)$ to $w_c \tilde{c}$ thus results in an approximate restriction of $r(t)$ to an $N - 1$ -dimensional hyperplane with $c(t) = o_c r(t) \approx \tilde{c}$ (Fig. 4b). The resulting trajectory is for task (i) a stable periodic orbit that generates the desired signal, because the vector field projected to the $c(t) = \tilde{c}$ -hyperplane is similar to the vector field projected to the $c(t) = \tilde{c}$ -hyperplanes embedding nearby pretrained periodic orbits (Fig. 4c).

Discussion and conclusion. We have introduced a scheme how neural networks can quickly learn dynamics without changing their weights and without requiring a teacher during testing. It relies on a weight-learned mutual association, quasi an entanglement, between contexts and targets. This enables the latter to fix the former during dynamical learning and vice versa during testing.

Previous approaches to supervised dynamical learning with continuous signal space required a form of the teaching signal also during testing. They further differ in network architecture, learning algorithm, task and/or assumption of discrete time from ours [10–23, 27, 74–76]. In networks with external input unseen, interpolating input can lead to interpolating dynamics [27, 77]. In contrast,

our networks *learn* new dynamics, by imitation.

Our scheme is conceptually independent of the network and weight-learning model. The pretraining implements a form of structure learning, i.e. learning of the structure underlying a task family [6, 78]. Animals and humans employ it frequently, but little is known about its neurobiology. We thus realize it by a simple reservoir computing scheme with FORCE learning [25, 27]. We checked that we can use biologically more plausible weight perturbation learning for a simple fixed point learning task [27].

Dynamical learning is biologically plausible: it is naturally local, causal and does not require fast synaptic weight updates. Continuous supervision could be generated by an inverse model [79] and might be replaceable by a sparse, partial signal. Our dynamical learning is fast [27] (cf. also [8, 10, 11, 13, 14, 75]). Even for more complicated tasks convergence requires only a few multiples of a characteristic time scale of the dynamics. Further, we find robustness against changes in network and task parameters [27]. The above points suggest a high potential of our scheme for applications in biology, physics and engineering such as neuromorphic computing and the prediction of chaotic systems [27].

We thank Paul Züge for fruitful discussions, the German Federal Ministry of Education and Research (BMBF) for support via the Bernstein Network (Bernstein Award 2014, 01GQ1710) and the European Union’s Horizon 2020 research and innovation programme for support via the Marie Skłodowska-Curie Grant No 754411.

-
- [1] P. Dayan and L. F. Abbott, *Theoretical Neuroscience: Computational and Mathematical Modeling of Neural Systems* (MIT Press, Cambridge, 2001).
- [2] W. Gerstner, W. M. Kistler, R. Naud, and L. Paninski, *Neuronal Dynamics - From Single Neurons to Networks and Models of Cognition* (Cambridge University Press, Cambridge, 2014).
- [3] M. G. Perich, J. A. Gallego, and L. E. Miller, “A neural population mechanism for rapid learning,” *Neuron* **100**, 964–976.e7 (2018).
- [4] S. Thrun and L. Pratt, eds., *Learning to Learn* (Springer US, 1998).
- [5] Joaquin Vanschoren, “Meta-Learning: A Survey,” arXiv:1810.03548 (2018).
- [6] B. J. Lansdell and K. P. Kording, “Towards learning-to-learn,” arXiv:1811.00231 (2018).
- [7] Y. Duan, J. Schulman, X. Chen, P. L. Bartlett, I. Sutskever, and P. Abbeel, “RL²: Fast Reinforcement Learning via Slow Reinforcement Learning,” arXiv:1611.02779 (2016).
- [8] J. X. Wang, Z. Kurth-Nelson, D. Kumaran, D. Tirumala, H. Soyer, J. Z. Leibo, D. Hassabis, and M. Botvinick, “Prefrontal cortex as a meta-reinforcement learning system,” *Nat. Neurosci.* **21**, 860–868 (2018).
- [9] A. Nagabandi, I. Clavera, S. Liu, R. S. Fearing, P. Abbeel, S. Levine, and C. Finn, “Learning to Adapt: Meta-Learning for Model-Based Control,” arXiv:1803.11347 (2018).
- [10] L. A. Feldkamp, G. V. Puskorius, and P. C. Moore, “Adaptation from fixed weight dynamic networks,” in *Proceedings of International Conference on Neural Networks (ICNN’96)*, Vol. 1 (1996) pp. 155–160 vol.1.
- [11] L. A. Feldkamp, G. V. Puskorius, and P. C. Moore, “Adaptive behavior from fixed weight networks,” *Information Sciences* **98**, 217–235 (1997).
- [12] A. S. Younger, P. R. Conwell, and N. E. Cotter, “Fixed-weight on-line learning,” *IEEE Transactions on Neural Networks* **10**, 272–283 (1999).
- [13] S. Hochreiter, A. S. Younger, and P. R. Conwell, “Learning to Learn Using Gradient Descent,” in *Artificial Neural Networks — ICANN 2001*, Lecture Notes in Computer Science, edited by G. Dorffner, H. Bischof, and K. Hornik (Springer Berlin Heidelberg, 2001) pp. 87–94.
- [14] A. S. Younger, S. Hochreiter, and P. R. Conwell, “Meta-learning with backpropagation,” in *IJCNN’01. International Joint Conference on Neural Networks. Proceedings (Cat. No.01CH37222)* (2001) pp. 2001–2006 vol.3.
- [15] L. A. Feldkamp, D. V. Prokhorov, and T. M. Feldkamp, “Simple and conditioned adaptive behavior from Kalman filter trained recurrent networks,” *Neural Networks* **16**, 683–689 (2003).
- [16] R. A. Santiago, “Context discerning multifunction networks: Reformulating fixed weight neural networks,” in *2004 IEEE International Joint Conference on Neural Networks (IEEE Cat. No.04CH37541)*, Vol. 1 (2004) pp. 189–194.
- [17] M. Lukosevicius, *Echo State Networks with Trained Feedbacks*, Tech. Rep. (Jacobs University Bremen, 2007).
- [18] A. Santoro, S. Bartunov, M. Botvinick, D. Wierstra, and T. Lillicrap, “Meta-Learning with Memory-Augmented Neural Networks,” in *International Conference on Machine Learning* (2016) pp. 1842–1850.
- [19] G. Bellec, D. Salaj, A. Subramoney, R. Legenstein, and W. Maass, “Long short-term memory and learning-to-learn in networks of spiking neurons,” arXiv:1803.09574 (2018).
- [20] L. A. Feldkamp and G. V. Puskorius, “Training of robust neural controllers,” in *Proceedings of 1994 33rd IEEE Conference on Decision and Control* (1994) pp. 2754–2759 vol.3.
- [21] L. A. Feldkamp and G. V. Puskorius, “Training controllers for robustness: Multi-stream DEKF,” in *Proceedings of 1994 IEEE International Conference on Neural Networks (ICNN’94)*, Vol. 4 (IEEE, Orlando, FL, USA, 1994) pp. 2377–2382.
- [22] L. A. Feldkamp and G. V. Puskorius, “Fixed-weight controller for multiple systems,” in *Proceedings of International Conference on Neural Networks (ICNN’97)* (1997) pp. 773–778 vol.2.
- [23] M. Oubbati and G. Palm, “A neural framework for adaptive robot control,” *Neural Computing and Applications* **19**, 103–114 (2010).
- [24] H. Jaeger, M. Lukosevicius, D. Popovici, and U. Siewert, “Optimization and applications of echo state networks with leaky-integrator neurons,” *Neural Networks* **20**, 335–352 (2007).
- [25] D. Sussillo and L. F. Abbott, “Generating coherent patterns of activity from chaotic neural networks,” *Neuron*

- 63**, 544–557 (2009).
- [26] D. Sussillo and O. Barak, “Opening the black box: Low-dimensional dynamics in high-dimensional recurrent neural networks,” *Neural Comput.* **25**, 626–649 (2013).
- [27] See Supplemental Material [url] for further detail on the tasks, analyses of the learning performance, pretraining using weight perturbation and an extended discussion, which includes Refs. [28–65].
- [28] D. V. Buonomano and M. M. Merzenich, “Temporal information transformed into a spatial code by a neural network with realistic properties.” *Science* **267**, 1028–1030 (1995).
- [29] P. F. Dominey, “Complex sensory-motor sequence learning based on recurrent state representation and reinforcement learning.” *Biol. Cybern.* **73**, 265–274 (1995).
- [30] M. B. Westover, C. Eliasmith, and C. H. Anderson, “Linearly decodable functions from neural population codes,” *Neurocomputing* **44–46**, 691–696 (2002).
- [31] T. Miconi, “Biologically plausible learning in recurrent neural networks reproduces neural dynamics observed during cognitive tasks,” *eLife* **6**, e20899 (2017).
- [32] B. DePasquale, C. J. Cueva, K. Rajan, G. S. Escola, and L. F. Abbott, “Full-force: A target-based method for training recurrent networks,” *PLoS One* **13**, e0191527 (2018).
- [33] <https://github.com/chklos/dynamical-learning>.
- [34] O. Schütze, X. Esquivel, A. Lara, and C. A. C. Coello, “Using the averaged hausdorff distance as a performance measure in evolutionary multiobjective optimization.” *IEEE Trans. Evolutionary Computation* **16**, 504–522 (2012).
- [35] H. Jaeger, “Controlling Recurrent Neural Networks by Conceptors,” arXiv:1403.3369 (2014).
- [36] H. Jaeger, “Using Conceptors to Manage Neural Long-Term Memories for Temporal Patterns,” *Journal of Machine Learning Research* **18**, 1–43 (2017).
- [37] A. Dembo and T. Kailath, “Model-free distributed learning,” *IEEE Transactions on Neural Networks* **1**, 58–70 (1990).
- [38] M. Jabri and B. Flower, “Weight perturbation: an optimal architecture and learning technique for analog VLSI feedforward and recurrent multilayer networks,” *IEEE Transactions on Neural Networks* **3**, 154–157 (1992).
- [39] G. Cauwenberghs, “A Fast Stochastic Error-Descent Algorithm for Supervised Learning and Optimization,” in *Advances in Neural Information Processing Systems*, Vol. 5 (1993) pp. 244–251.
- [40] H. S. Seung, “Learning in Spiking Neural Networks by Reinforcement of Stochastic Synaptic Transmission,” *Neuron* **40**, 1063–1073 (2003).
- [41] C. Beer and O. Barak, “One step back, two steps forward: interference and learning in recurrent neural networks,” arXiv:1805.09603 (2018).
- [42] D. P. Kingma and J. Ba, “Adam: A Method for Stochastic Optimization,” in *Proceedings of the 3rd International Conference on Learning Representations*, Vol. 3 (2015).
- [43] R. L. Redondo and R. G. M. Morris, “Making memories last: the synaptic tagging and capture hypothesis,” *Nat. Rev. Neurosci.* **12**, 17–30 (2011).
- [44] Z. Yu, D. Kappel, R. Legenstein, S. Song, F. Chen, and W. Maass, “CaMKII activation supports reward-based neural network optimization through Hamiltonian sampling,” arXiv:1606.00157 (2016).
- [45] W. C. Abraham, “Metaplasticity: tuning synapses and networks for plasticity,” *Nat. Rev. Neurosci.* **9**, 387 (2008).
- [46] G. V. Puskorius and L. A. Feldkamp, “Neurocontrol of nonlinear dynamical systems with Kalman filter trained recurrent networks,” *IEEE Trans. Neural Netw.* **5**, 279–297 (1994).
- [47] E. D. Sontag, “Neural Nets as Systems Models and Controllers,” in *Proc. Seventh Yale Workshop on Adaptive and Learning Systems* (1992) pp. 73–79.
- [48] K-I. Funahashi and Y. Nakamura, “Approximation of dynamical systems by continuous time recurrent neural networks,” *Neural Networks* **6**, 801–806 (1993).
- [49] K-K. K. Kim, E. R. Patrón, and R. D. Braatz, “Standard representation and unified stability analysis for dynamic artificial neural network models,” *Neural Networks* **98**, 251–262 (2018).
- [50] N. E. Cotter and P. R. Conwell, “Fixed-weight networks can learn,” in *1990 IJCNN International Joint Conference on Neural Networks* (1990) pp. 553–559 vol.3.
- [51] N. E. Cotter and P. R. Conwell, “Learning algorithms and fixed dynamics,” in *IJCNN-91-Seattle International Joint Conference on Neural Networks* (1991) pp. 799–801 vol.1.
- [52] S. Lim and M. S. Goldman, “Balanced cortical microcircuitry for maintaining information in working memory,” *Nat. Neurosci.* **16**, 1306–1314 (2013).
- [53] W. Maass, P. Joshi, and E. D. Sontag, “Computational aspects of feedback in neural circuits,” *PLOS Comput. Biol.* **3**, e165 (2007).
- [54] R. Pascanu and H. Jaeger, “A neurodynamical model for working memory,” *Neural Networks* **24**, 199–207 (2011).
- [55] J. A. Gallego, M. G. Perich, L. E. Miller, and S. A. Solla, “Neural manifolds for the control of movement,” *Neuron* **94**, 978–984 (2017).
- [56] E. Chicca, F. Stefanini, C. Bartolozzi, and G. Indiveri, “Neuromorphic electronic circuits for building autonomous cognitive systems,” *Proc. IEEE* **102**, 1367–1388 (2014).
- [57] F. Duport, A. Smerieri, A. Akrouf, M. Haelterman, and S. Massar, “Fully analogue photonic reservoir computer,” *Sci. Rep.* **6** (2016).
- [58] A. N. Tait, T. F. de Lima, E. Zhou, A. X. Wu, M. A. Nahmias, B. J. Shastri, and P. R. Prucnal, “Neuromorphic photonic networks using silicon photonic weight banks,” *Sci. Rep.* **7** (2017).
- [59] P. Antonik, M. Haelterman, and S. Massar, “Brain-inspired photonic signal processor for generating periodic patterns and emulating chaotic systems,” *Phys. Rev. Appl.* **7** (2017).
- [60] D. Thalmeier, M. Uhlmann, H. J. Kappen, and R.-M. Memmesheimer, “Learning universal computations with spikes,” *PLoS Comput. Biol.* **12**, e1004895 (2016).
- [61] C. D. Schuman, T. E. Potok, R. M. Patton, J. D. Birdwell, M. E. Dean, G. S. Rose, and J. S. Plank, “A survey of neuromorphic computing and neural networks in hardware,” arXiv:1705.06963 (2017).
- [62] J. Pathak, B. Hunt, M. Girvan, Z. Lu, and E. Ott, “Model-Free Prediction of Large Spatiotemporally Chaotic Systems from Data: A Reservoir Computing Approach,” *Phys. Rev. Lett.* **120**, 024102 (2018).
- [63] R. S. Zimmermann and U. Parlitz, “Observing spatio-temporal dynamics of excitable media using reservoir computing,” *Chaos* **28**, 043118 (2018).
- [64] K. K. Sreenivasan and M. D’Esposito, “The what, where

- and how of delay activity,” *Nat. Rev. Neurosci.* **20**, 466–481 (2019).
- [65] K. Oberauer, “Is rehearsal an effective maintenance strategy for working memory?” *Trends Cogn. Sci.* **23**, 798–809 (2019).
- [66] H. Jaeger and H. Haas, “Harnessing nonlinearity: Predicting chaotic systems and saving energy in wireless communication,” *Science* **304**, 78–80 (2004).
- [67] W. Maass, T. Natschläger, and H. Markram, “Real-time computing without stable states: A new framework for neural computation based on perturbations,” *Neural Comput.* **14**, 2531–2560 (2002).
- [68] M. Lukosevicius, H. Jaeger, and B. Schrauwen, “Reservoir computing trends,” *Künstl. Intell.* **26**, 365–371 (2012).
- [69] M. Y. Ismail and J. C. Principe, “Equivalence between RLS algorithms and the ridge regression technique,” in *Proc. Systems and Computers Conf. Record of The Thirtieth Asilomar Conf. Signals* (1996) pp. 1083–1087 vol.2.
- [70] V. Mante, D. Sussillo, K. V. Shenoy, and W. T. Newsome, “Context-dependent computation by recurrent dynamics in prefrontal cortex.” *Nature* **503**, 78–84 (2013).
- [71] G. Hennequin, T. P. Vogels, and W. Gerstner, “Optimal control of transient dynamics in balanced networks supports generation of complex movements,” *Neuron* **82**, 1394–1406 (2014).
- [72] L. F. Abbott, B. DePasquale, and R-M. Memmesheimer, “Building functional networks of spiking model neurons,” *Nat. Neurosci.* **19**, 350–355 (2016).
- [73] L. F. Abbott, K. Rajan, and H. Sompolinsky, “Neuronal variability and its functional significance,” (Oxford University Press, 2010) Chap. Interactions between Intrinsic and Stimulus Evoked Activity in Recurrent Neural Networks, pp. 65–82.
- [74] M. Oubbati, P. Levi, and M. Schanz, “Meta-Learning for Adaptive Identification of Non-Linear Dynamical Systems,” in *Proceedings of the 2005 IEEE International Symposium on, Mediterrean Conference on Control and Automation Intelligent Control, 2005.* (2005) pp. 473–478.
- [75] H. Jaeger and D. Eck, “Can’t get you out of my head: A connectionist model of cyclic rehearsal,” in *Modeling Communication with Robots and Virtual Humans* (Springer, Berlin, Heidelberg, 2008) pp. 310–335.
- [76] F. wyffels, J. Li, T. Waegeman, B. Schrauwen, and H. Jaeger, “Frequency modulation of large oscillatory networks,” *Biol. Cybern.* **108**, 145–157 (2014).
- [77] K. J. Boström, H. Wagner, M. Prieske, and M. de Lussanet, “Model for a flexible motor memory based on a self-active recurrent neural network,” *Human Movement Science* **32**, 880 – 898 (2013).
- [78] D. A. Braun, C. Mehring, and D. M. Wolpert, “Structure learning in action,” *Behavioural Brain Research* **206**, 157–165 (2010).
- [79] M. I. Jordan and D. E. Rumelhart, “Forward models: Supervised learning with a distal teacher,” *Cognitive Science* **16**, 307–354 (1992).

Dynamical learning of dynamics
– **Supplemental Material** –

Christian Klos,¹ Yaroslav Felipe Kalle Kossio,¹ Sven
Goedeke,¹ Aditya Gilra,^{1,2} and Raoul-Martin Memmesheimer¹

¹*Neural Network Dynamics and Computation,
Institute of Genetics, University of Bonn, Bonn, Germany.*

²*Department of Computer Science, and Neuroscience Institute, University of Sheffield, Sheffield, UK.*

I. RESERVOIR COMPUTING AND FORCE LEARNING

Reservoir computing has been introduced several times at different levels of elaborateness and in different flavors, in machine learning and in neuroscience [1–4]. A reservoir computer consists of a high-dimensional, nonlinear dynamical system, the reservoir or liquid, and a comparably simple readout. The reservoir, often a recurrent neural network, “echoes” the input in a complicated, nonlinear way; it acts like a random filter bank with finite memory as each of its units generates a nonlinearly filtered version of the current input and its recent past while forgetting more remote inputs [1, 3–5]. The simple, often linear readout can then be weight-trained to extract the desired results while the reservoir remains static. Only a fraction of the neural network weights are therefore used for task-related adaptation.

We use a reservoir computing scheme for pretraining, see main text. The output weights of our networks, the weights o_z and o_c to z and c , learn online according to the FORCE rule [6], which is well suited for reservoir computers with output feedback [7]. This is because it assumes fast learning of the output weights with a powerful algorithm and thereby ensures that the output and thus the feedback input always match the desired ones up to a small error. The recurrent network is thus largely driven by the correct feedback signals and generates appropriate dynamics already during training. The remaining fluctuations are intrinsically generated and therefore efficiently immunize the system against fluctuations that will occur during testing, leading to dynamically stable generation of desired dynamics. The output weights are trained using the supervised recursive least-squares algorithm. This higher order algorithm provides a least-squares optimal, usually regularized result given the past network states and the targets. Concretely, the version used in ref. [6] and in our article starts the recursion with $o_{z,ij}(0)$ and $o_{c,ij}(0)$ for the signal and context output weights and with an $N \times N$ matrix $P(0) = \alpha^{-1}I$, where I is the identity matrix and α^{-1} acts as a learning rate parameter. In learning step n at time t_n the output weights $o_z(n)$ and $o_c(n)$ and the matrix $P(n)$ are recursively updated via

$$o_{z,ij}(n) = o_{z,ij}(n-1) - g_j(n)\varepsilon_i(t_n), \quad (\text{S1})$$

$$o_{c,ij}(n) = o_{c,ij}(n-1) - g_j(n)e_i(t_n), \quad (\text{S2})$$

$$P(n) = (I - g(n)r^T(t_n))P(n-1), \quad (\text{S3})$$

where T denotes transposition, $r(t_n)$ the outputs of the neurons at time t_n and $\varepsilon(t) = z(t) - \tilde{z}(t)$ and $e(t) = c(t) - \tilde{c}(t)$ the errors of the signal and the context. $g(n) = (1 + r^T(t_n)P(n-1)r(t_n))^{-1}P(n-1)r(t_n)$ specifies the learning rates of $o_{z,ij}$ and $o_{c,ij}$. They depend on the presynaptic neuron j and on the dynamical history of the entire reservoir, which renders the algorithm causal but non-local. The recursion ensures

that $o_z(n)$ and $o_c(n)$ minimize the “ridge regression” error functions

$$E_{z,i}(n) = \sum_{k=1}^n \left(\sum_j o_{z,ij}(n) r_j(t_k) - \tilde{z}_i(t_k) \right)^2 + \alpha \sum_{j=1}^N (o_{z,ij}(n) - o_{z,ij}(0))^2, \quad (\text{S4})$$

$$E_{c,i}(n) = \sum_{k=1}^n \left(\sum_j o_{c,ij}(n) r_j(t_k) - \tilde{c}_i(t_k) \right)^2 + \alpha \sum_{j=1}^N (o_{c,ij}(n) - o_{c,ij}(0))^2, \quad (\text{S5})$$

i.e. the individual signal and context errors are kept small with weights that ideally do not deviate far from the initial ones (weight regularization) [8]. The non-locality and the assumed fast weight changes are considered biologically implausible [6, 9].

II. ADDITIONAL DETAIL ON THE APPLICATIONS

In the following, we detail the parameters, setups and targets used in the different applications. We denote the duration of the pretraining phase by t_{wlearn} . Each training period (individual target presentation) in it lasts for t_{stay} . If not mentioned otherwise, in the beginning of each period until t_{fb} the network receives error input $\varepsilon(t)$ and the context signal evolves freely. Thereafter, $w_\varepsilon \rightarrow 0$ and $c(t)$ is fixed to its target value. The intervals between updates of the output weights have length dt for task (ii) and random lengths with an average of 0.5 for the other tasks [10]. The parameter of the FORCE rule is $\alpha = 1$. Dynamical learning lasts for t_{learn} . During dynamical learning, we determine \bar{c} by averaging the context signal with an exponentially forgetting kernel ($\tau_{\text{forget}} = 50$ for task (v) and $\tau_{\text{forget}} = 5$ for the other tasks). Testing lasts for t_{test} .

In all applications, recurrent weights A_{ij} are set to zero with probability $1 - p$. Nonzero weights are drawn from a Gaussian distribution with mean 0 and variance $\frac{g^2}{pN}$, where $g = 1.5$ [6]. We draw the feedback weights $w_{z,ij}$, $w_{c,ij}$ and the input weights $w_{\varepsilon,ij}$, $w_{u,ij}$ from a uniform distribution between $-\tilde{w}$ and \tilde{w} , set all initial output weights $o_{z,ij}(0)$ and $o_{c,ij}(0)$ to 0 and draw the biases b_i from a uniform distribution between -0.2 and 0.2 . The number of external inputs is N_u . We use the standard Euler method for our simulations, with an integration time step of $dt = 0.1$, except for Figs. 4 and S7, where we use $dt = 0.01$ and $dt = 0.025$, respectively. See [11] for example code for task (i).

Further settings in the individual tasks are as follows:

Task (i): $N = 500, N_z = 1, N_c = 1, N_u = 0, p = 0.1, \tilde{w} = 1, t_{\text{stay}} = 500, t_{\text{fb}} = 100, t_{\text{wlearn}} = 50000, t_{\text{learn}} = 50, t_{\text{test}} = 5000$. The network learns to generate sinusoidal oscillations with period T . The family of target trajectories is $\tilde{z}(t; T) = 5 \sin(\frac{2\pi}{T}t)$. We use three different teacher trajectories for pretraining, with periods $T = 10, 15, 20$ and corresponding context targets $\tilde{c} = 2, 2.5, 3$. The target of dynamical learning in Figs. 2a and S8 has $T = 12.5$.

Task (ii): $N = 500\text{--}3000, N_z = 1, N_c = 1, N_u = 0, p = 0.1, \tilde{w} = 1, t_{\text{stay}} = 500, t_{\text{fb}} = 100, t_{\text{wlearn}} = 50000, t_{\text{learn}} = 100, t_{\text{test}} = 500$. We do not update the output weights during a time interval of 20 at the beginning of each training period. The network learns to generate a superposition of two Fourier series with weighting factor λ . The family of target trajectories is $\tilde{z}(t; \lambda) = (1 - \lambda)\tilde{z}_1(t; \lambda) + \lambda\tilde{z}_2(t; \lambda)$ with $\tilde{z}_l(t) = \frac{1}{C_l}(\frac{\tilde{a}_{l,0}}{2} + \sum_{o=1}^O \tilde{a}_{l,o} \sin(\frac{2\pi o}{T(\lambda)}t + \tilde{\varphi}_{l,o}))$, $l = 1, 2$, and $T(\lambda) = (1 - \lambda)T_1 + \lambda T_2$. We draw the $\tilde{a}_{l,0}$, $\tilde{a}_{l,o}$, $\tilde{\varphi}_{l,o}$ and T_l from uniform distributions between -10 and 10 , 0 and 10 , 0 and 2π , and 20 and 50 , respectively. C_l is drawn from a uniform distribution to normalize the maximal value of $|\tilde{z}_l(t)|$ to a random value between 3 and 7. We use seven different teacher trajectories for pretraining, with weighting factors λ distributed equidistantly between 0 and 1. The corresponding context targets are distributed equidistantly between 2 and 3. The target of dynamical learning in Fig. 2c has $N = 2000, O = 6, \lambda = \frac{7}{12}$.

Task (iii): $N = 1000, N_z = 1, N_c = 2, N_u = 0, p = 0.2, \tilde{w} = 1, t_{\text{stay}} = 500, t_{\text{fb}} = 100, t_{\text{wlearn}} = 50000, t_{\text{test}} = 1000$. The network learns to generate a superposition of sinusoidal oscillations with amplitude a and period T . The family of target trajectories is $\tilde{z}(t; a, T) = a \left(\sin(\frac{2\pi}{T}t) + \cos(\frac{4\pi}{T}t) \right)$. We use sixteen different teacher trajectories for pretraining, with four amplitudes a distributed equidistantly between 3 and 7 and four periods T distributed equidistantly between 10 and 20. The corresponding context targets are distributed equidistantly between 2 and 3 for both parameters. The target of dynamical learning in Figs. 3a and S8 has $a = 5$ and $T = 15$.

Task (iv): $N = 500, N_z = 3, N_c = 1, N_u = 0, p = 0.1, \tilde{w} = 1, t_{\text{stay}} = 200, t_{\text{fb}} = 100, t_{\text{wlearn}} = 50000, t_{\text{learn}} = 50, t_{\text{test}} = 1000$. The network learns to generate a constant output positioned on a curve in three-dimensional space parameterized by s . The family of target trajectories (fixed points) is $\tilde{z}(t; s) = \left(\frac{s^3}{2} + s_{\text{off}}, 2(s - \frac{1}{2})^2 + s_{\text{off}}, \frac{s}{2} + s_{\text{off}} \right)$, where the offset $s_{\text{off}} = 2.5$ ensures that the network feedback is strong enough to entrain the reservoir network. We use ten different teacher trajectories for pretraining with parameters s chosen between 0 and 1 such that the corresponding $\tilde{z}(t; s)$ lie equidistantly on the target curve $\{\tilde{z}(t; s) | s \in [0, 1]\}$. The corresponding context targets are distributed equidistantly between 2 and 3. The targets of dynamical learning in Fig. 3b have $s = 0.10$ and $s = 0.92$.

Task (v): $N = 1000, N_z = 1, N_c = 1, N_u = 1, p = 0.2, \tilde{w} = 2, t_{\text{stay}} = 1000, t_{\text{wlearn}} = 30000, t_{\text{learn}} = 200, t_{\text{test}} = 500$. We choose τ_i from a uniform distribution between 0.3 and 2.5. During pretraining, we always provide error input $\varepsilon(t)$ to the network and do not fix $c(t)$, i.e. $t_{\text{fb}} = t_{\text{stay}} = 1000$. The network learns to predict the angle of a driven overdamped pendulum with mass m . The family of target dynamical systems is given by $\dot{\tilde{z}}(t) = F(\tilde{z}(t), u(t); m) = -m \sin(\tilde{z}(t)) + u(t) - \exp((\tilde{z}(t) - 0.65\pi)/0.65\pi) + \exp(-(\tilde{z}(t) + 0.65\pi)/0.65\pi)$. The last two terms provide a soft barrier preventing the pendulum from undergoing full rotations. During pretraining and dynamical learning, the pendulum is driven by low-pass filtered white noise $\dot{u}_{\text{wlearn}}(t) = -u_{\text{wlearn}}(t) + 0.2dW/dt$ (see Fig. S5b), which allows a comprehensive sampling of the pendulum's dynamics. During testing the pendulum is driven by a triangular wave with unit amplitude and period $T = 50$. We use three different teacher dynamical systems for pretraining, with $m = 0.5, 1.0, 1.5$ and corresponding context targets $\tilde{c} = 0.7, 0.95, 1.2$. The targets of dynamical learning in Fig. 3c,d have $m = 0.8$ (continuous trace) and $m = 1.2$ (dashed trace).

Task (vi): $N = 1000, N_z = 3, N_c = 1, N_u = 0, p = 0.1, \tilde{w} = 2, t_{\text{stay}} = 1000, t_{\text{fb}} = 100, t_{\text{wlearn}} = 50000, t_{\text{learn}} = 50, t_{\text{test}} = 10000$. The network learns a Lorenz system with dissipation parameter β . During pretraining, we always provide error input $\varepsilon(t)$ to the network, but fix $c(t)$ after t_{fb} . The family of target dynamical systems is given by $\dot{\tilde{z}}(t) = F(\tilde{z}(t); \beta) = F_{\text{Lorenz}}(C_{\text{Lorenz}}\tilde{z}(t); \beta)/(C_{\text{Lorenz}}\tau_{\text{Lorenz}})$, where $C_{\text{Lorenz}} = 40$ and $\tau_{\text{Lorenz}} = 20$ determine the spatial and temporal scale of the dynamics and $F_{\text{Lorenz}}(x(t); \beta) = (\sigma(x_2 - x_1), x_1(\rho - x_3) - x_2, x_1x_2 - \beta x_3)$ is the vector field of the standard Lorenz sys-

tem, with $\sigma = 10$ and $\rho = 70$. We use four teacher dynamical systems for pretraining, with parameters β distributed equidistantly between 2 and 6 and corresponding context targets distributed equidistantly between 2 and 3. The target of dynamical learning in Fig. 3e,f and S8 has $\beta = 4$.

III. QUANTIFICATION OF LEARNING PERFORMANCE

To quantify the performance of our model, we measure for each application the errors between signal outputs and targets during testing, for different network instances and targets. Except for task (vi), we compute the testing error as the root-mean-square error between signal output and target during a period of length 50 in the middle of the testing phase. The measure is chosen to ignore phase shifts that occur over long testing times, as they are unavoidable in periodic autonomous dynamics (tasks (i,ii)), due to the accumulation of small errors in the period.

Task (i): Fig. S1a shows the testing error for the learning of sinusoidal oscillations. It is small for targets with periods within and slightly beyond the range spanned and interspersed by pretrained targets. Fig. S1b shows the good agreement between the periods of the output signals and the targets. We determine the periods from the maxima of the output signals' power spectra, after discarding the initial interval of length 100 of the testing phase to allow for equilibration.

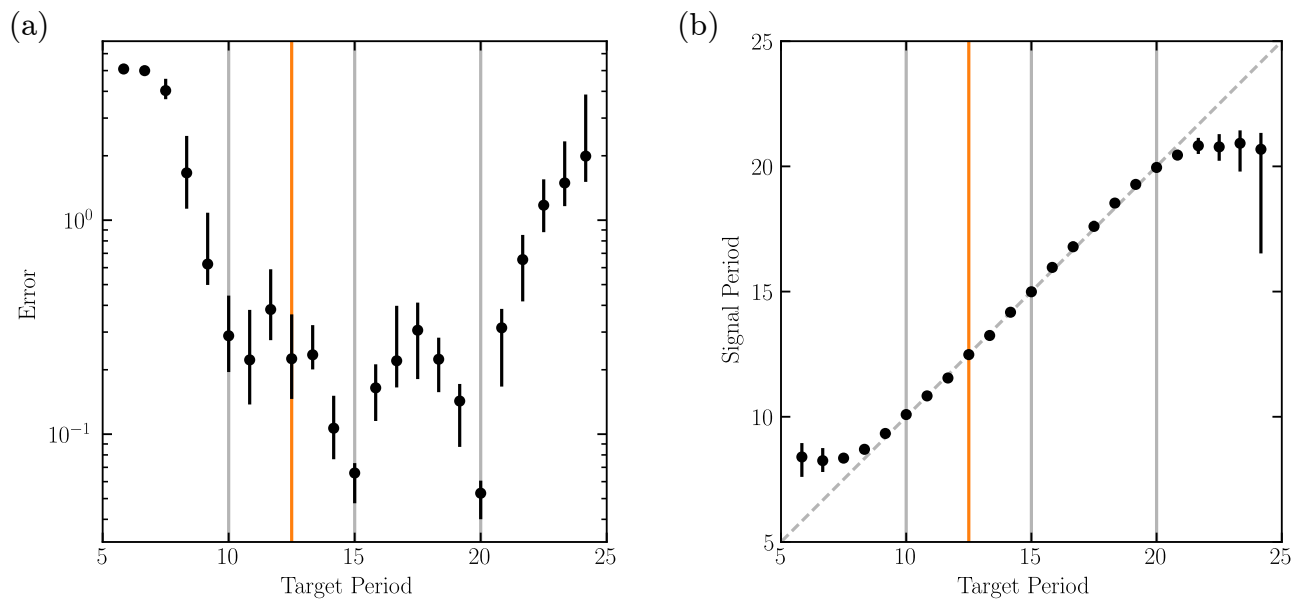


Figure S1. Quality of dynamical learning of the sinusoidal oscillations in task (i). (a) Testing error between signal output and target and (b) period of the signal output, as a function of the period of the target. Vertical gray lines indicate the periods of the pretrained targets and vertical orange lines indicate the period of the target used in Fig. 2a. Dots show median value and errorbars represent the interquartile range between first and third quartile, using 10 network instances.

Task (ii): Fig. S2 shows the testing error for four different combinations of network size N and order O together with the signal and target in time and frequency domain for example instances of task (ii), i.e., for specific realizations of the random Fourier series described above. The testing error is low within the

range of pretrained weighting factors, especially for the targets used during pretraining.

Task (iii): Fig. S3a shows the testing error for the learning of superpositions of sines. Again, the error is low within and slightly beyond the range of the parameters of the pretrained targets. Similarly, the averaged local maxima of the signal outputs agree well with the averaged local maxima of their targets, Fig. S3b. The measurement of maxima starts at time 100 after the beginning of testing.

Task (iv): Fig. S4a shows the testing error for the learning of fixed points. It is low for target positions within and slightly beyond the range of the positions of the pretrained targets. Fig. S4b shows signal outputs for different targets dynamically learned by a single network instance.

Task (v). Fig. S5a shows the testing error for the learning of driven overdamped pendulums. It is small for pendulums with masses within and slightly beyond the range spanned and interspersed by pretrained pendulums. Fig. S5b illustrates the dynamical learning and testing phases.

Task (vi): Since the Lorenz system is chaotic for most of the parameter range that we consider, the signal output trajectory quickly deviates from the target system’s trajectory during testing. This holds also if the network approximates the target dynamical system well. Hence, instead of using the root-mean-square error, we compute the testing error as the discrepancy of the limit set M_{net} generated by the network and the limit set M_{tar} generated by the target dynamics. For the comparison, we use the Averaged Hausdorff Distance [12],

$$d_{\text{AHD}}(M_{\text{net}}, M_{\text{tar}}) = \max \left[\frac{1}{|M_{\text{net}}|} \sum_{m_{\text{net}} \in M_{\text{net}}} d(m_{\text{net}}, M_{\text{tar}}), \frac{1}{|M_{\text{tar}}|} \sum_{m_{\text{tar}} \in M_{\text{tar}}} d(m_{\text{tar}}, M_{\text{net}}) \right], \quad (\text{S6})$$

$$d(m, M) = \min_{m' \in M} \| m - m' \|,$$

which is robust against outliers. Fig. S6a shows that the testing error is low within the range of parameters β spanned and interspersed by pretrained targets. In addition, we find that the relation between subsequent maxima of the z-coordinate of the signal output correctly forms the shape of a tent for most tested parameters (Fig. S6b). The behavior of our model also reproduces a bifurcation occurring for large β : The target Lorenz system changes from chaotic behavior to fixed point behavior for the largest value of β we consider. Our networks dynamically learn to generate the fixed point dynamics from this target, although they were only pretrained in the chaotic regime. We note that some network instances, for example the one shown in Fig. S6b, generate fixed point behavior during testing, if the target has the second largest value of β and is thus still chaotic. However, also in these cases the signal output converges to one of the two fixed points appearing for the largest β . This suggests that due to a shift in the averaged context parameter, the dynamical regime beyond the bifurcation is generated during testing.

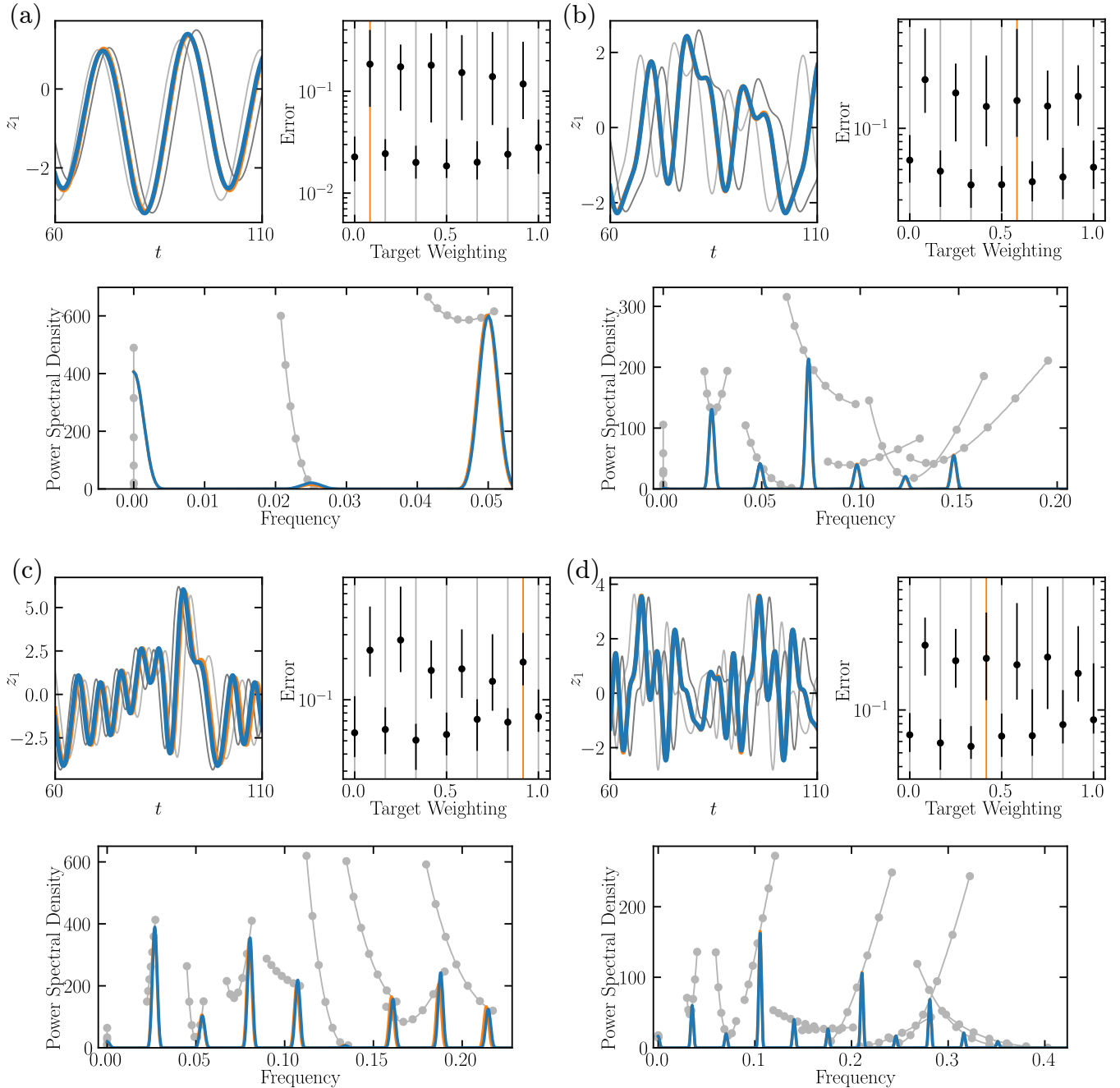


Figure S2. Quality of dynamical learning of the superposition of Fourier series in task (ii). (a) $N = 1000, O = 2$ (a, top left) Signal (blue) and target (orange) together with the two closest pretrained dynamics (gray) during testing after dynamical learning of an unseen target. (a, bottom) Power spectral density of signal (blue) and target (orange) during testing. Gray lines show the power of the individual Fourier components of the target family within the range of pretrained targets. Gray dots indicate the targets used during pretraining. (a, top right) Testing error between signal output and target as a function of the target weighting factor. Vertical gray lines indicate the weighting factors of the pretrained targets and vertical orange lines indicate the weighting factors of the targets used in the other subpanels. Dots show median value and errorbars represent the interquartile range between first and third quartile, using 40 network instances and random Fourier series. (b-d) Same as (a) but with (b) $N = 2000, O = 6$, (c) $N = 2500, O = 8$, (d) $N = 3000, O = 10$.

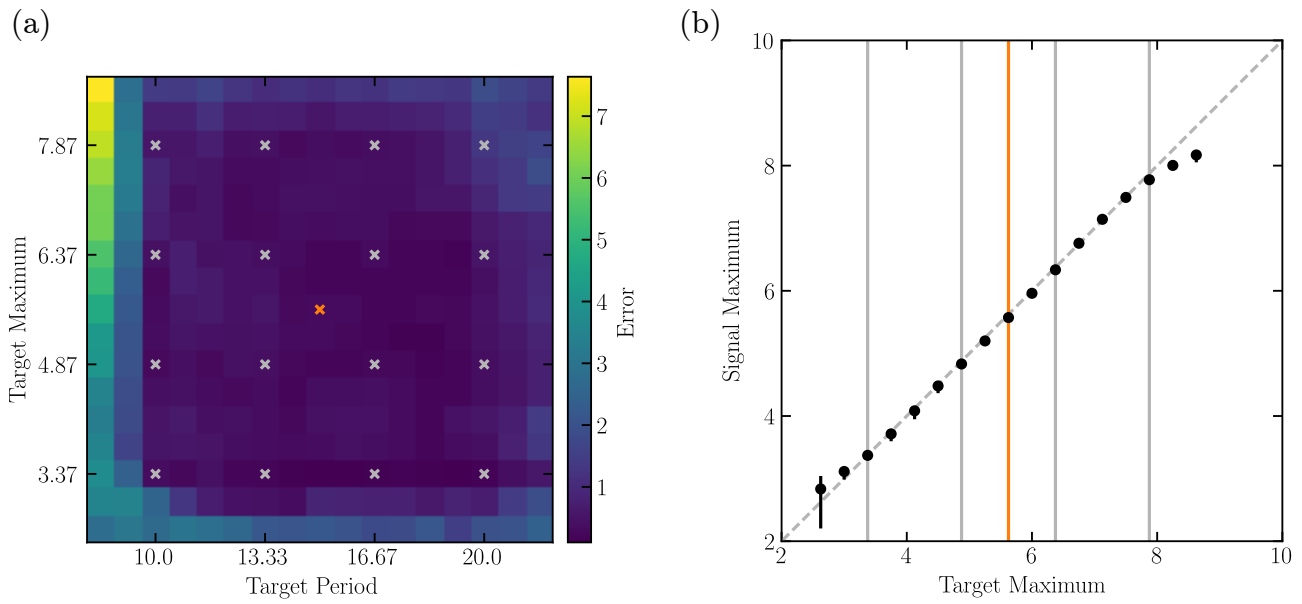


Figure S3. Quality of dynamical learning of the superpositions of sines in task (iii). (a) Median testing error between signal output and target as a function of the maximum and the period of the target function. Gray crosses indicate parameters of the pretrained targets and the orange cross indicates the parameters used in Fig. 3a. (b) Averaged local maxima of the signal output as a function of the averaged local maxima of the target, for a target period of $T = 15$. Vertical gray lines indicate the maxima of the pretrained targets and the vertical orange line indicates the maximum of the target used in Fig. 3a. Dots show median value and errorbars represent the interquartile range between first and third quartile. Results in (a) and (b) are obtained using 10 network instances for each parameter pair.

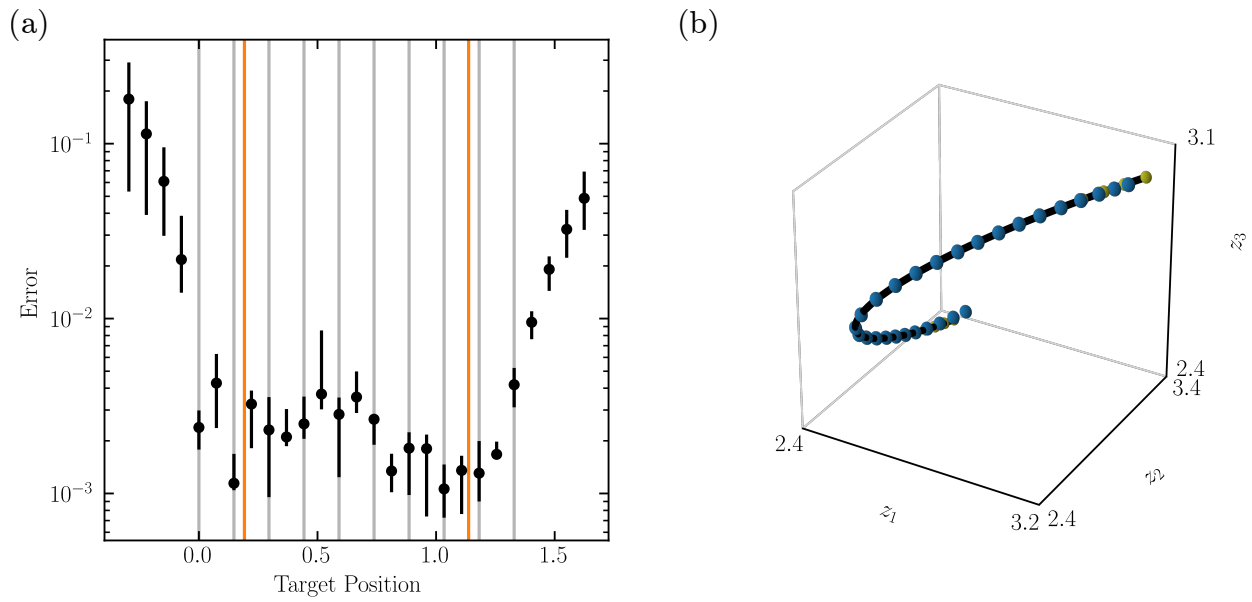


Figure S4. Quality of dynamical learning of the fixed points in task (iv). (a) Testing error between signal output and target as a function of the target position. Vertical gray lines indicate the positions of the pretrained targets and vertical orange lines indicate the positions of the targets used in Fig. 3b. Dots show median value and errorbars represent the interquartile range between first and third quartile, using 10 network instances. (b) Single network instance learning the same set of dynamical learning targets as in (a). Blue spheres indicate the last signal outputs during testing after the different instances of dynamical learning. Yellow spheres indicate the position of the corresponding targets. They are mostly covered by blue spheres, except in the regions of larger error. The black tube shows the curve $\tilde{z}(t; s)$ on which the targets lie.

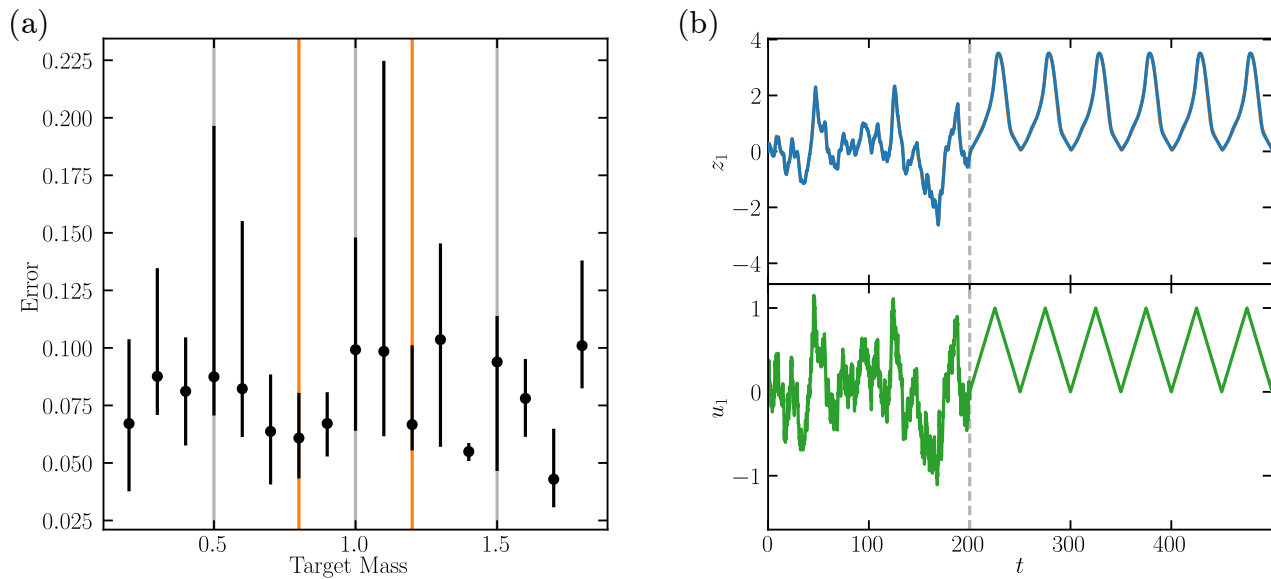


Figure S5. Quality of dynamical learning of the overdamped pendulums in task (v). (a) Error between signal output and target, as a function of the target pendulum's mass. Vertical gray lines indicate the masses of the pretrained targets and vertical orange lines indicate the masses of the targets used in Fig. 3d,e. Dots show median value and errorbars represent the interquartile range between first and third quartile, using 10 network instances. (b) Dynamical learning and testing. The network and the target receive the same low-pass filtered white noise as input drive during dynamical learning and triangular wave input during testing (lower subpanel). The network response (upper subpanel, blue trace) agrees well with the response of the target (upper subpanel, orange trace, nearly completely covered by the blue trace).

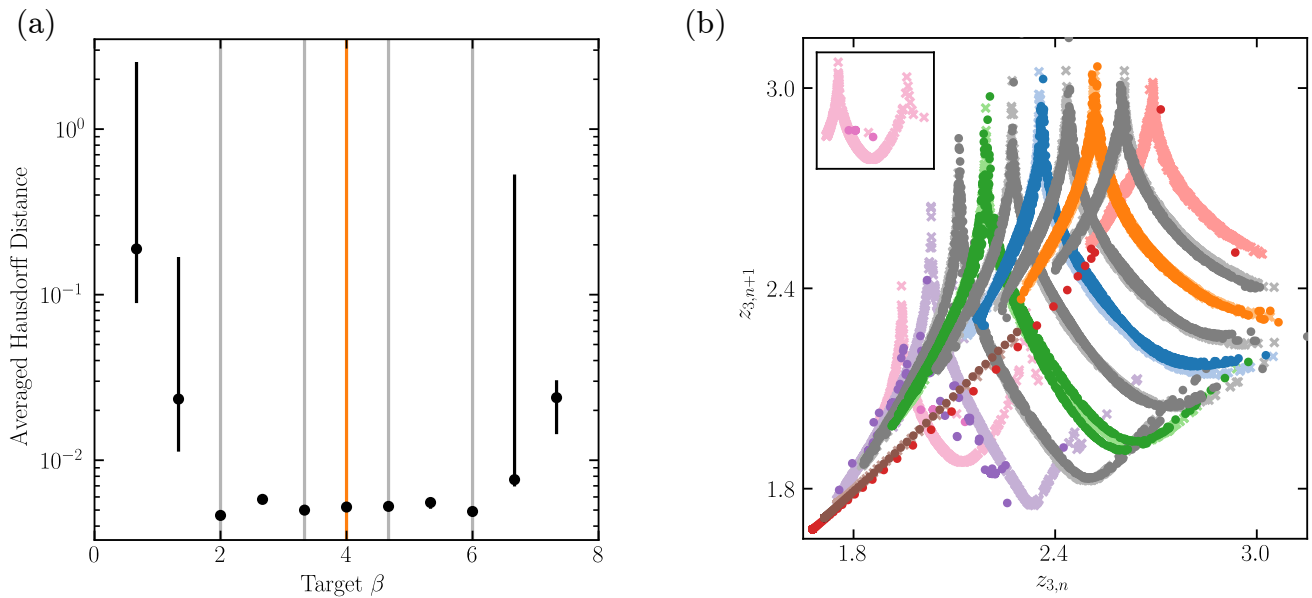


Figure S6. Quality of dynamical learning of the Lorenz systems in task (vi). (a) Testing error comparing the limit sets of signal output and target, as a function of the target's parameter β . Vertical gray lines indicate the parameters of the pretrained targets and the vertical orange line indicates the parameter of the target used in Fig. 3e,f. Dots show median value and errorbars represent the interquartile range between first and third quartile, using 10 network instances. (b) Tent maps of subsequent maxima in the z-coordinate for the signal output (dots, colored differently for different targets) and for the target dynamics (crosses, light coloring alike corresponding dots). The parameters β of the targets are the same as in (a). Dynamical learning of all targets with a single network instance. Blue data correspond to the signal and target used in Fig. 3e,f; gray data indicate pretrained targets. Tent maps of the target dynamics move from bottom left to top right for increasing β except for the largest β (brown, bottom left), for which the target dynamics converge to a fixed point. Inset show close-up of results for the smallest considered value of β . The signal output goes to a fixed point for the two largest, but also for the smallest considered value of β , leading to a focusing of the maxima relation to a small region.

IV. ANALYSIS OF DYNAMICAL LEARNING OF CHAOTIC DYNAMICS

To show that the mechanisms underlying dynamical learning and testing that we worked out using task (i) in the main text also hold for a qualitatively different, chaotic system, Fig. S7 analyzes them for task (vi). As expected, we observe that during dynamical learning, the error feedback drives the dynamics towards an orbit generalizing the pretrained ones and keeps it there. During testing, the network generalizes the pretrained characteristics to autoencode c such that the dynamics stay near the \bar{c} -plane in r -space when the feedback $w_c c$ is clamped to $w_c \bar{c}$. The trajectory is for task (vi) usually chaotic and generates the desired output signal, because the vector field projected to the $c(t) = \bar{c}$ -hyperplane inter- or extrapolates nearby vector fields of other c -hyperplanes, which embed pretrained orbits generating Lorenz dynamics with neighboring parameters.

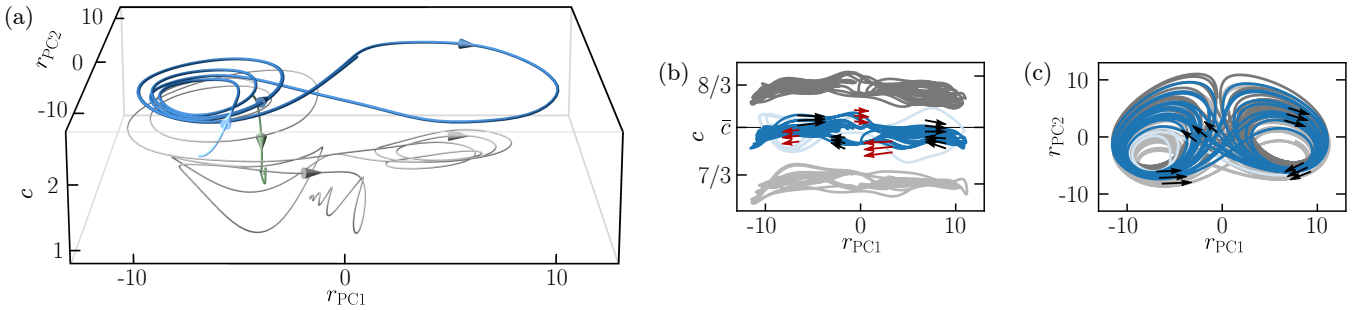


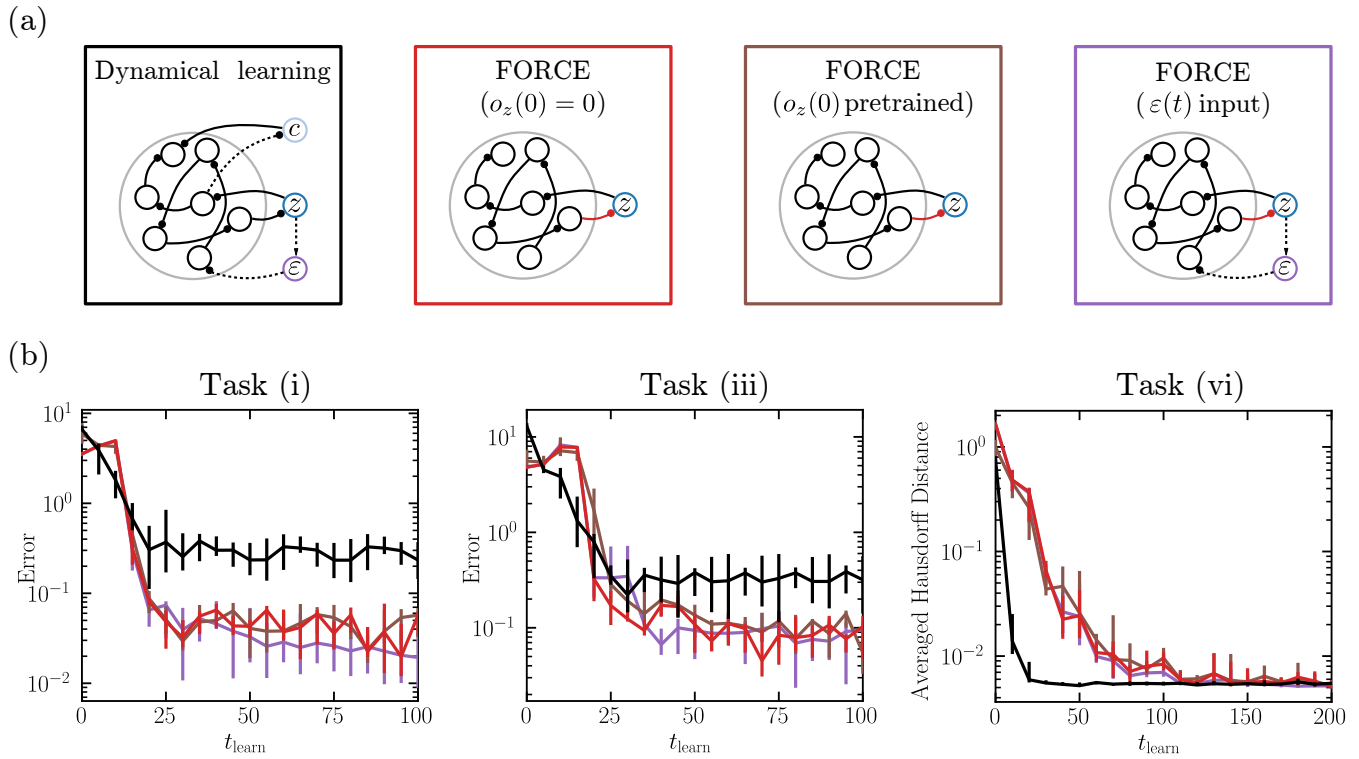
Figure S7. Recurrent network dynamics during dynamical learning (a) and testing (b,c) of task (vi), in c, r_{PC1}, r_{PC2} -coordinates (see Fig. 4 for task (i)). (a) During dynamical learning, the error input drives the network to an orbit whose signal output approximates the desired Lorenz system and keeps it there (light blue and blue trajectories). Without input, the dynamics converge to a stable fixed point, after a transient that yields a Lorenz system-like signal (gray). Freezing $\tilde{z}(t) = \tilde{z}(t_0)$ drives the dynamics quickly to a fixed point (green). (b) During testing, the assumed orbit (blue) resembles the error driven one in the c - $r_{PC,1}$ -plane (light blue, closest pretrained orbits with $c(t)$ fixed to their \tilde{c} : gray). The constant feedback \bar{c} prevents the dynamics to leave the region where $c(t) \approx \bar{c}$, compare $\dot{r}(r)$ (black vectors, r on/nearby trajectory) with $\dot{r}(r)$ for variable feedback $c(t)$ (red vectors). (c) All four orbits are similar in the $r_{PC,1}$ - $r_{PC,2}$ -plane, since the dynamically learned orbit has a similar projected vector field (black vectors) as the nearby pretrained ones.

V. LEARNING SPEED OF DYNAMICAL LEARNING

In the following we quantitatively assess the speed of dynamical learning. We compare it with that of standard FORCE weight-learning, which uses reservoirs with only a signal output $z(t)$ and output weight-learning. As example tasks we consider learning of the sinusoidal oscillation, main text task (i), of the superposition of sines, main text task (iii), and of the Lorenz system, main text task (vi). The reservoirs for standard FORCE learning have our standard parameters, except that the biases are drawn from a uniform distribution between -5 and 5. Further, the output weight-learning parameters are adapted; we apply weight updates on every integration time step and set α to 0.001. Both changes improve performance and are for some combinations of configuration and task even necessary for convergence. We consider three different configurations of standard FORCE learning (Fig. S8a): First, the typical configuration of a reservoir without input and initialization of o_z to 0. In the second configuration o_z is initialized instead to the signal output weights obtained at the end of pretraining for dynamical learning. This accounts for the possibility that these output weights are beneficial initial conditions for weight-learning and that our structural learning facilitates subsequent FORCE learning despite the lack of context input, which was present during pretraining. In the third configuration o_z is initialized to 0 and the reservoir receives an error input $\varepsilon(t) = z(t) - \tilde{z}(t)$ during learning, because this might also facilitate FORCE learning. To evaluate performance after different learning durations, we compute testing errors as described in Sec. III. As usual, we stop weight modifications and, if present, error input during testing. For a fair comparison, for dynamical learning with $t_{\text{learn}} = 0$ we fix the context to 0.

We find that dynamical learning is similarly fast or faster than FORCE (Fig. S8b). For tasks (i) and (iii), both dynamical learning and FORCE learning converge within approximately two periods of the target dynamics ($T = 12.5$ and $T = 15$). FORCE learning converges to smaller errors. For task (vi), dynamical learning converges in about five cycles (maxima of the z -coordinate) of the target system. FORCE learning is about five times slower and yields similar errors. The similar convergence speed of the first two configurations in all considered tasks indicates that FORCE weight-learning does not profit from our form of pretraining.

Taken together, we observe that dynamical learning converges within a few characteristic timescales of the target dynamics and is thus on par with FORCE learning for simple and faster converging for complex tasks. This held for both the standard and the hand-tuned parameter sets. The observation is plausible since for complicated tasks FORCE learning needs to gather information that dynamical learning already possesses due to the previous pretraining. It is especially interesting because dynamical learning may be considered biologically plausible and because FORCE is a recommended reservoir computing scheme [7].



VI. ROBUSTNESS OF LEARNING PERFORMANCE

To check the robustness of our dynamical learning scheme against changes in task family parameters, we determine its performance for different families of sinusoidal oscillations, main text task (i). Specifically, we vary the number of pretrained targets, the amplitude of the oscillations, the difference between the maximal and minimal period of the pretrained targets (period range) as well as the minimal period of the weight-learned targets. For each combination of these task family parameters, we pretrain the networks as before. Afterwards, we dynamically learn a set of targets with periods ranging from the smallest to the largest pretrained period, where the period increases by one between neighboring targets. We compute a normalized error for each target and take the average to quantify the performance of the network for the considered task family. The normalized error is the root-mean-square error during a period in the middle of the testing phase, with length three times the target period, divided by the corresponding root-mean-square error assuming that the signal output is zero.

To compute and interpret the errors in high-dimensional parameter space, we cut out slices where we keep all but at most two of the task family parameters at their standard values specified in Sec. II. We find that dynamical learning works robustly for large parameter regions. In particular, the number of targets and the period range can often be changed over an order of magnitude, see Fig. S9. Increasing the network size to 1000 neurons and the number of pretrained targets to five instead of three further increases robustness against changing other parameters, see Fig. S10. Taken together, we may conclude that our scheme works well for a wide range of task families.

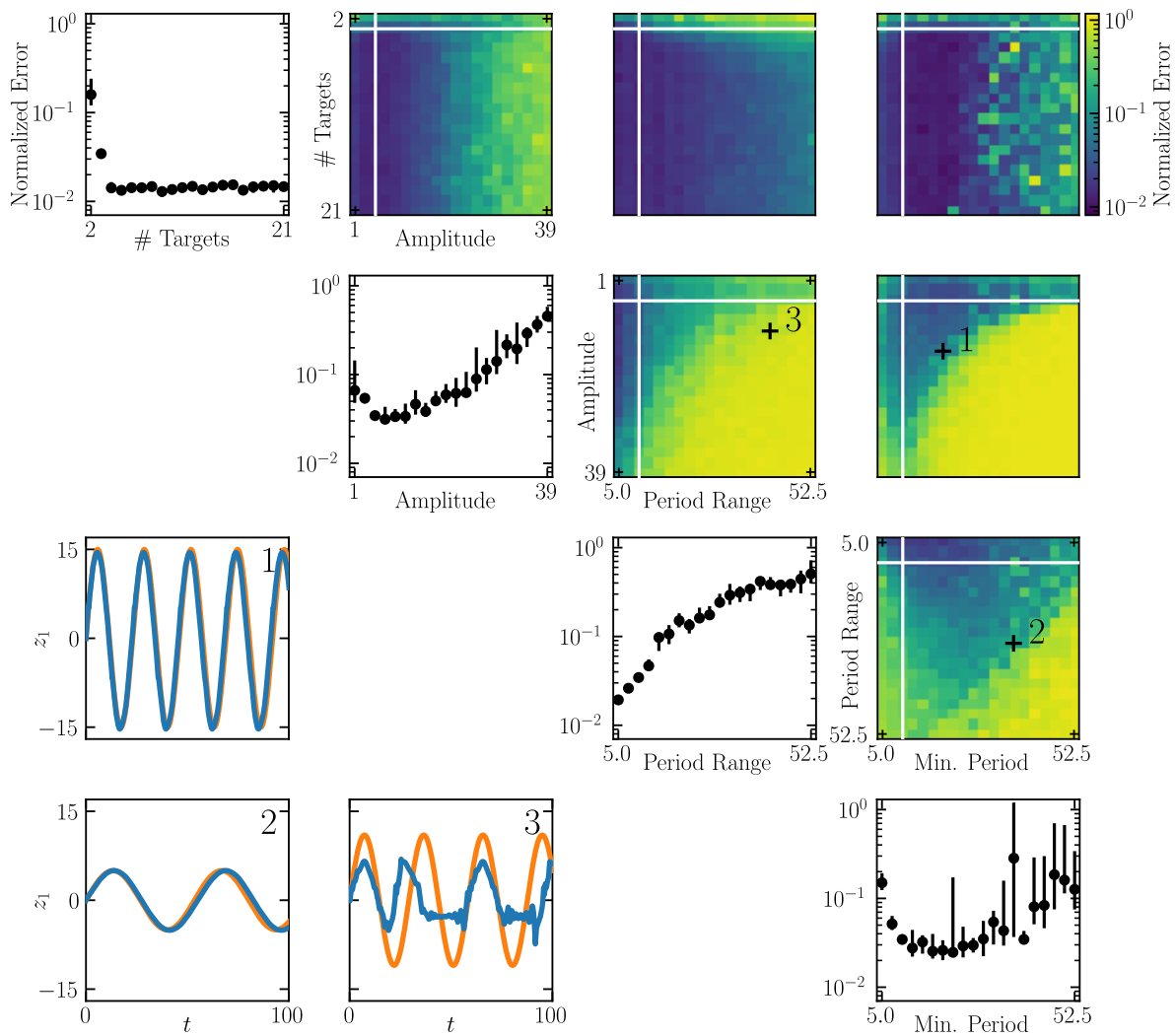


Figure S9. Performance over a broad range of task family parameters. Panels on and above the diagonal show the average normalized errors taken over sets of testing targets. All but the indicated parameters are set to their standard values. White lines in panels above the diagonal indicate the parameter values of the one-dimensional slices shown on the diagonal. Dots and color represent median value and errorbars in panels on the diagonal represent the interquartile range between first and third quartile, using 10 network instances. Panels below the diagonal show representative dynamically learned example signal outputs (blue) and corresponding targets (orange) for the three different parameter combinations indicated by numbered crosses in the panels above the diagonal.

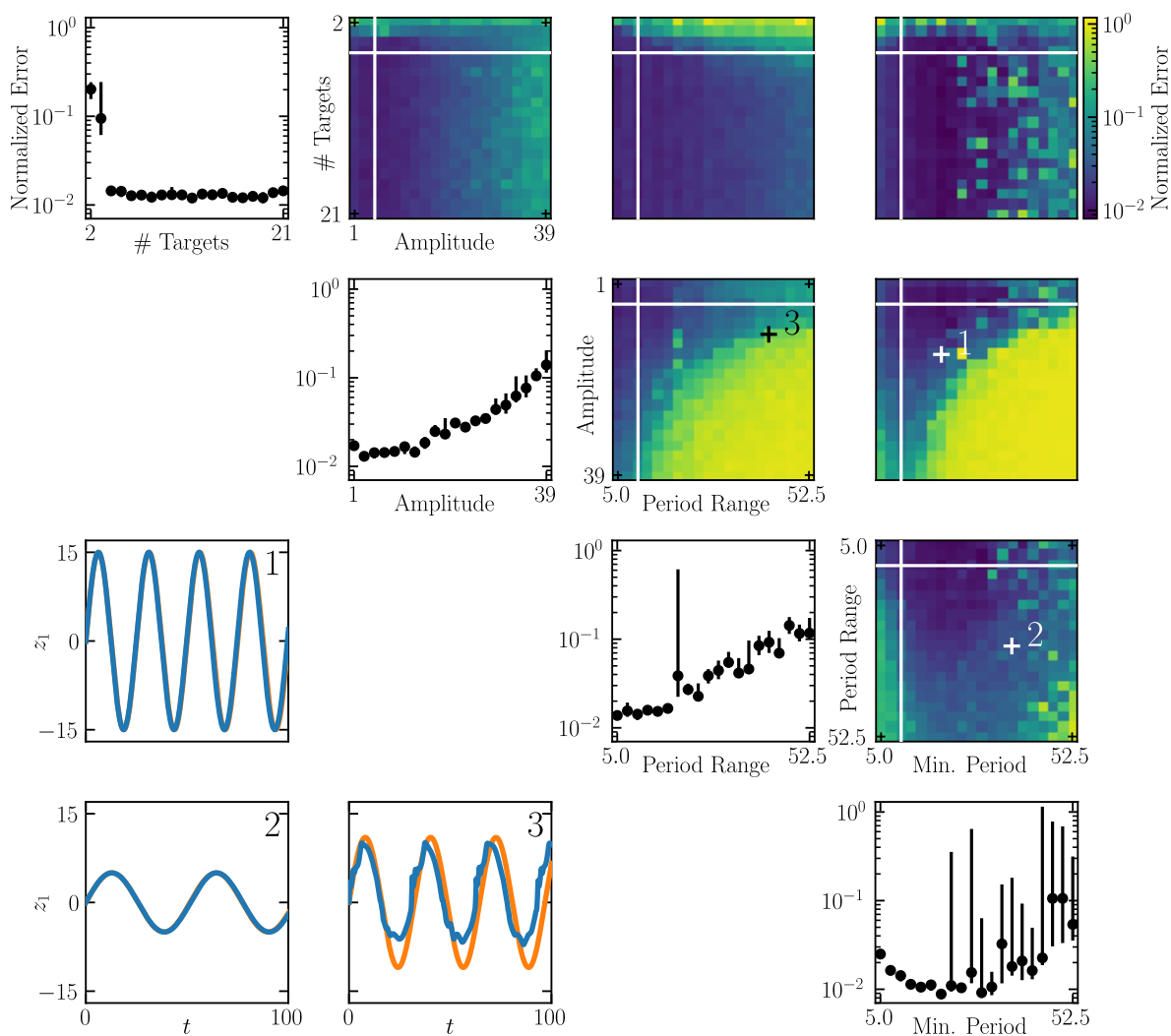


Figure S10. Same as Fig. S9 for networks with 1000 neurons and five pre-trained targets unless the number of pre-trained targets is varied.

VII. INDUCTION OF UNSEEN SIGNAL OUTPUTS BY A CONTEXT-LIKE EXTERNAL INPUT

We test whether changing a context-like input $u_c(t)$ allows to generate sinusoidal oscillations with previously unseen frequencies. Like $c(t)$, $u_c(t)$ connects to the neurons in the network with a weight matrix w_c . However, $u_c(t)$ is never generated by a network output, but a purely external input. There is no further context variable $c(t)$ and no error input $\varepsilon(t)$ in the network. Apart from this, the network is setup like in task (i). The output weights w_z are learned using the FORCE rule, similar to pretraining in task (i): during each training period, we teach the network to generate a sinusoidal oscillation $\tilde{z}(t; T)$ with a period $T = 10, 15, 20$, in response to a constant $u_c(t) = 2, 2.5, 3$, analogous to teacher forcing with \tilde{c} . We find that the system can interpolate between the pretrained output signals, if driven by previously unseen $u_c(t)$, cf. Fig. S11. See ref. [13] for a similar finding when morphing between conceptor weight matrices. (The recent ‘conceptor’ approach fixes reservoir dynamics by weight changes Jaeger [13, 14].)

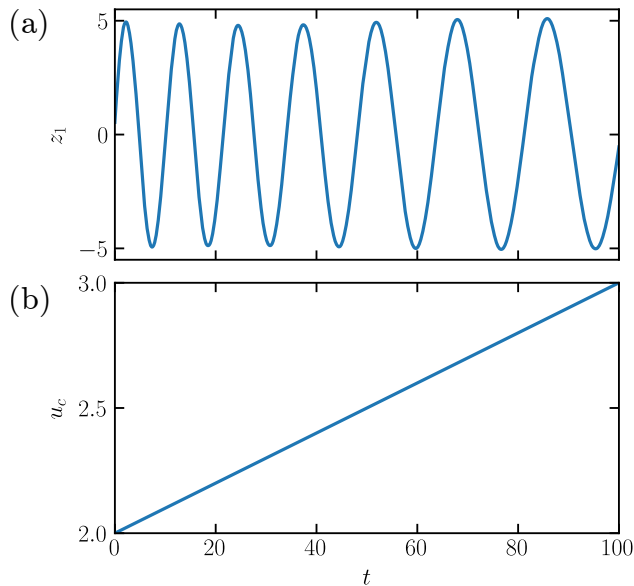


Figure S11. Induction of unseen signal outputs by a context-like external input. The network has been trained similar to pretraining in task (i) to generate sinusoidal oscillations with three different frequencies in response to three constant external context inputs $u_c(t)$. After training, the weights are fixed and the network receives a continuously rising $u_c(t)$ (b). This results in a sinusoidal signal output with continuously rising period, which interpolates between the trained signals (a).

VIII. PRETRAINING WITH WEIGHT PERTURBATION

Introduction. Throughout the article reservoir computing with FORCE learning is used for pretraining, see main text and Supplemental Material Secs. I-VII. In the following we show dynamical learning of simple tasks in networks that are pretrained with a biologically more plausible rule. Specifically, we use reservoir computing with weight perturbation [15–18] to learn network structures that enable the dynamical learning of fixed points in two-dimensional space. We note that the direct application of a recent node perturbation scheme [9] to the output or all neurons was hindered by difficulties with learning multiple targets (cf. also [19]). Weight perturbation is, in short, a local reinforcement learning rule that consists of three steps: (i) randomly perturbing the connection weights, (ii) comparing the obtained reward with the reward expected without perturbation, and (iii) changing the connection weights into the direction (opposite direction) of the perturbation if the actual reward is higher (lower) than the expected one.

Structure learning with weight perturbation. We use batch learning, i.e the pretraining phase consists of N_{trials} trials, each of which is comprised of the presentation of all N_{tar} pretraining members of the task family $\tilde{z}(t; s)$ for a time t_{stay} . The signal output weights o_z learn as follows: At the beginning of trial n , the weights $o_{z,ki}(n-1)$ from the end of the previous trial receive small perturbations $\Delta o_{z,ki}^{\text{pert}}(n)$ [17]. The perturbations are drawn from a normal distribution with zero mean and standard deviation σ . We define the reward $R_z(n)$ as the negative sum of the mean squared errors between the signals and their targets during an evaluation period that starts t_{off} after the beginning of the trial. Further, we approximate the reward of the unperturbed network on the training batch by an exponentially weighted average $\bar{R}_z(n-1) = \alpha \bar{R}_z(n-2) + (1-\alpha)R_z(n-1)$ of previous rewards with timescale α [9]. This gives the estimate

$$G_{ki}(n) = \frac{\Delta o_{z,ki}^{\text{pert}}(n)}{\sigma^2} (R_z(n) - \bar{R}_z(n-1)) \quad (\text{S7})$$

for the weight gradient [17]. When we obtain the weight updates $\Delta o_{z,ki}(n)$ directly from this estimate, in our model we observe poor performance. It improves markedly when we combine the estimate with the Adam algorithm [20]. Adam introduces a momentum term $v_{ki}(n)$ and an individual learning rate $1/\sqrt{g_{ki}(n) + \mu}$ for each connection such that our weight update equations read

$$o_{z,ki}(n) = o_{z,ki}(n-1) + \Delta o_{z,ki}(n), \quad (\text{S8})$$

$$\Delta o_{z,ki}(n) = \eta \frac{v_{ki}(n)}{\sqrt{g_{ki}(n) + \mu}}, \quad (\text{S9})$$

$$v_{ki}(n) = \beta v_{ki}(n-1) + (1-\beta)G_{ki}(n), \quad (\text{S10})$$

$$g_{ki}(n) = \gamma g_{ki}(n-1) + (1-\gamma)G_{ki}^2(n). \quad (\text{S11})$$

Here, η is the global learning rate, μ a constant preventing overly large weight updates and β and γ are the timescales of the exponential averaging of the momenta and the learning rates, respectively. Learning of the context output weights is implemented likewise.

Results. At the end of the pretraining trials, our networks have learned to produce (in response to the signal error input) signal and context outputs that are close to the pretrained targets within the evaluation period, see Fig. S12. The established underlying network structures also enable the network to dynamically learn previously unseen targets. Like for the differently pretrained networks in the main text and Supplemental Material Secs. I-VII, a short presentation of the (here constant) target signal via the error input teaches the network to imitate it and to choose an appropriate context. During a subsequent testing period, the network autonomously continues the desired signal stabilized by the fixated context. Fig. S13a shows the testing error after dynamical learning of different signals. It is low for target positions within and slightly beyond the range of the pretrained targets. Fig. S13b shows signal outputs, which were dynamically learned by a single network instance.

Discussion. We have shown that for a simple task pretraining can also be performed with a learning rule that satisfies main criteria for biological plausibility, as it is local and causal. Further, it relies on delayed, sparse rewards and updates the weights at a low rate at the end of a trial. It is biologically plausible that synapses tentatively change their weights and then consolidate or reverse the change, depending on reward [21]. To improve learning, we have employed momentum and individual, history dependent learning rates for each connection. Supported by experimental findings it has already been argued that the brain could realize learning with momentum [22]. Furthermore there is ample evidence for a complex history dependence of learning rates in individual synapses [23]. While our weight modifications do not rely on a continuous supervisory signal anymore, such a signal is still present in the error input, like during dynamical learning. Future work may investigate how it can be replaced by sparse supervision.

Task details. $N = 1000, N_z = 2, N_c = 1, N_u = 0, p = 0.1, \tilde{w} = 1, t_{\text{stay}} = 100, t_{\text{fb}} = 50, t_{\text{learn}} = 50, t_{\text{test}} = 1000, t_{\text{off}} = 25, N_{\text{trials}} = 10^5, N_{\text{tar}} = 5, \sigma = 10^{-4}, \alpha = 1/3, \beta = 0.99, \gamma = 0.99, \mu = 10^{-8}, \eta = 50 \times 10^{-5}$ for the first 5000 trials, $\eta = 10 \times 10^{-5}$ for trials 5000 to 50000, $\eta = 1 \times 10^{-5}$ afterwards. The model and application details described in the main text and in Sec. II also apply to the current setting, except for those concerning the weight-learning rule. At the beginning of each pretraining trial for each member of the batch we draw the initial activation variables x_i from a uniform distribution between -0.1 and 0.1 . The network learns to generate a constant output positioned on a curve in two-dimensional space parameterized by s . The family of target trajectories (fixed points) is $\tilde{z}(t; s) = \left(\frac{s^3}{2} + s_{\text{off}}, \frac{s}{2} + s_{\text{off}} \right)$, where the offset $s_{\text{off}} = 2.5$ ensures that the network feedback is strong enough to entrain the reservoir network. We use four different teacher trajectories for pretraining with parameters s chosen between 0 and 1 such

that the corresponding $\tilde{z}(t; s)$ lie equidistantly on the target curve $\{\tilde{z}(t; s) | s \in [0, 1]\}$. The corresponding context targets are distributed equidistantly between 2 and 3.

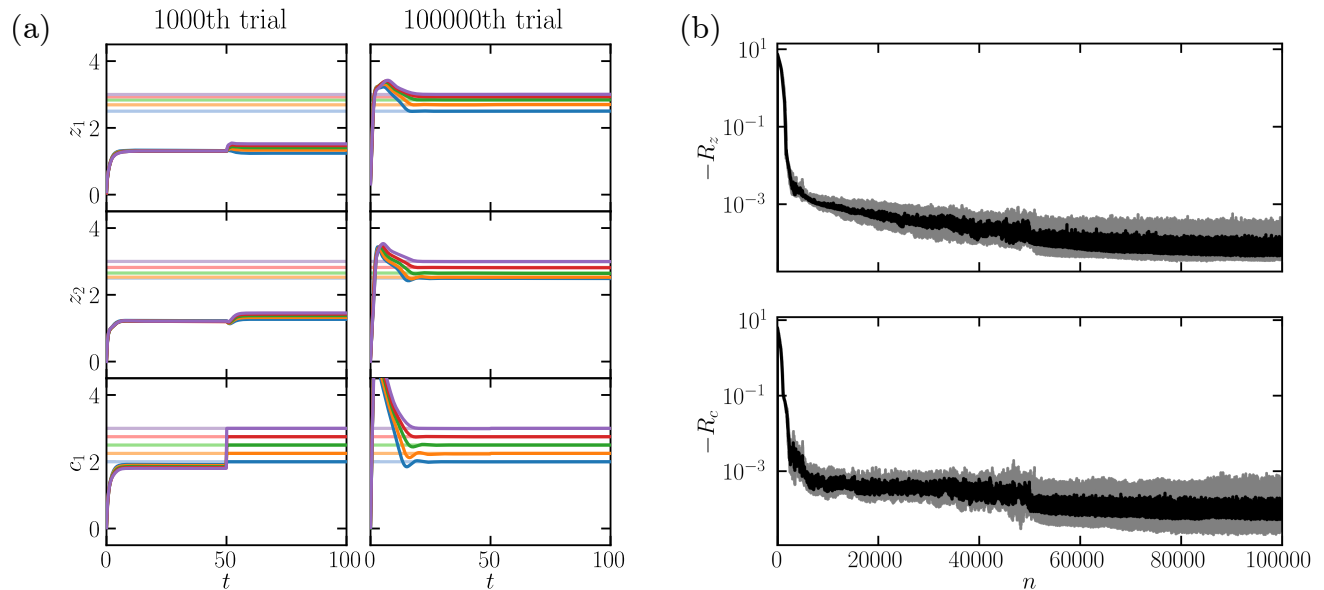


Figure S12. Pretraining using weight perturbation. (a) Signal and context outputs for the different batch members early (left) and late (right) during pretraining for a single network instance. In late trials the networks' error input induces a quick convergence of the outputs (strong colors) to their targets (light colors). At $t = 50$, the context variable is fixed to its desired value. (b) Negative reward for the signal (top) and context (bottom) output. Black line shows median value of 10 network instances and gray area indicates interquartile range between first and third quartile.

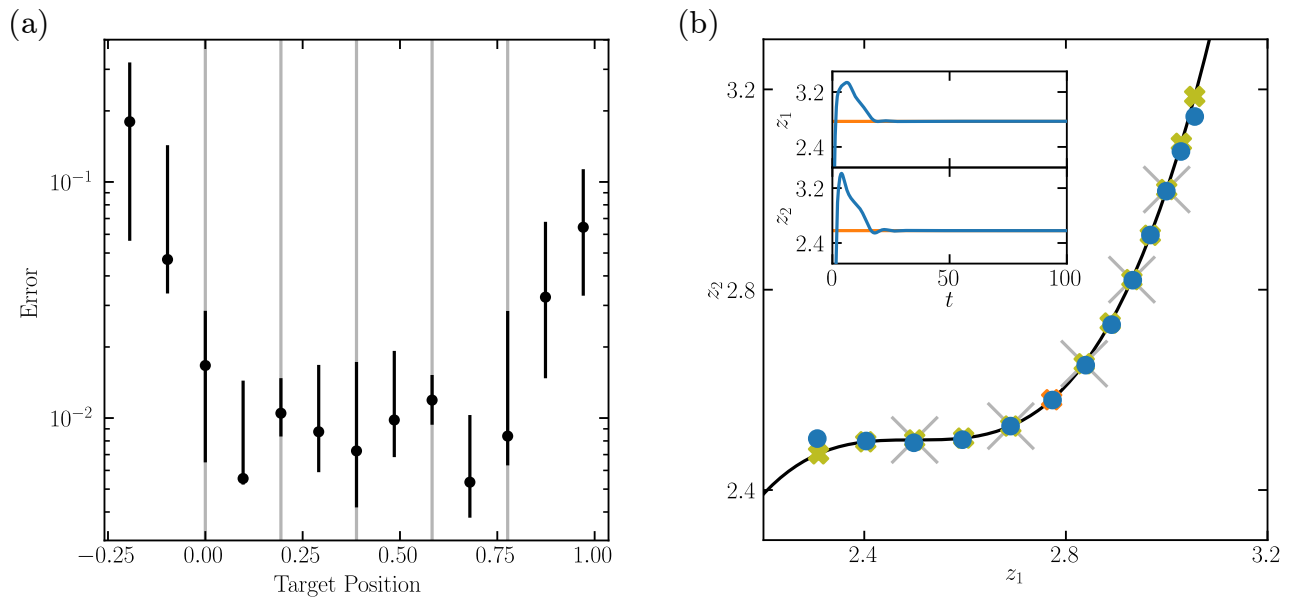


Figure S13. Quality of dynamical learning after pretraining with weight perturbation. (a) Testing error between signal output and target as a function of the target position. Vertical gray lines indicate the positions of the pretrained targets. Dots show median value and errorbars represent the interquartile range between first and third quartile, using 10 network instances. (b) Single network instance learning the same set of targets as in (a). The inset shows signal outputs (blue) versus time during dynamical learning and truncated testing periods for one of the targets (orange). In the main panel blue dots indicate the last signal outputs during testing. Yellow crosses indicate the position of the corresponding targets. They are mostly covered by blue dots, except in the regions of larger error. The orange cross indicates the position of the target shown in the inset. Gray crosses indicate the positions of the pretrained targets. The black line shows the curve $\tilde{z}(t; s)$ on which the targets lie.

IX. SUPPLEMENTARY DISCUSSION

We conclude with an extended discussion of our findings, previous literature and possible future applications. Overall, we have shown how neural networks can quickly learn trajectories and dynamical systems without changing their weights and without requiring a teacher during testing. During the pretraining (learning-to-learn), the networks are taught several dynamics from the same family as the later dynamically learned ones, as well as a corresponding constant context. The process is supervised by an error signal to the synapses and, part of the time, by an error input to the network. During dynamical learning, a short presentation of the latter alone suffices to teach the desired dynamics. The network then also generates a context, which fluctuates around some temporal mean. When subsequently testing the generation of the dynamics, the error input is removed and the context is fixed to its average, telling that the learned dynamics should be continued.

Our analysis indicates that the scheme works due to an interplay of generalization and stabilization: During pretraining, the networks adapt to perform a negative feedback/autoencoder task. During dynamical learning, they generalize this, by generating a new desired signal when receiving its error as input. Simultaneously they choose a consistent context. During testing, this context is externally kept constant, which stabilizes the learned signal. This is possible because a mutual association between contexts and targets has been weight-learned during pretraining.

Approaches to supervised dynamical learning in the literature consider the one-step prediction of time series [24, 25] and input-output maps [26–31], where the correct previous output is fed in. Other networks could adapt to provide negative feedback for control [32–35], a pretrained oscillation [36], periodic sequences of discrete states [37] or the parameters of a dynamical system [38]. The studies use simple recurrent neural networks [24, 25, 29, 32–35, 38], gated [27, 28, 30] or spiking ones [31], trained by backpropagation [27, 28, 30, 31] or extended Kalman filtering [24, 25, 32–35, 38–40]. The simple networks are similar to ours but use non-leaky neurons, different learning and often assume discrete time. To our knowledge, all the systems with continuous signal space were fed a form of the temporally variable teaching signal also during testing.

Earlier work showed that sufficiently large recurrent neural networks with static weights can approximate any smooth input-output dynamics relation with bound-restricted inputs for finite time [41–43]. This implies that a network with static weights can in principle approximate the output of another, weight-learning one. The static network’s dynamics thereby include the effects of the other network’s learning algorithm and thus learns dynamically [44, 45]. Our networks with static weights are not pretrained to approximate during dynamical learning the outputs of weight-learning networks. In particular they do not approximate the outputs of a FORCE weight-learning reservoir computer, as illustrated by the different

convergence properties in Suppl.-Fig. S8.

In our networks, fixing the intrinsically chosen context $c(t)$ indicates that the dynamics are to be continued. This is analogous to fixing the weights during testing in weight-learning paradigms. It is necessary to avoid convergence to other dynamics (if the system has discrete attractors) or diffusion (for marginally stable dynamics). The instruction to fix $c(t)$ is independent of the task and much simpler than task specific teacher and target signals. The constant $c(t)$ can be stored and kept up by biologically plausible circuits [46]. For long times, weight-learning may consolidate it. $c(t)$ may be understood as (continuous) memory variable [47, 48]. In contrast to previous ones it is neither a pure feedback output [47, 49] nor an external input (cf. Sec. VII and [50]) and it does not facilitate weight-learning [47, 49, 50]. One can also drive networks with external input such that unseen, interpolating input leads to interpolating dynamics (cf. Sec. VII and [51]). In contrast to such generalization, our networks learn their new dynamics by imitating a teacher. In particular, they adopt the phase of an oscillatory target.

Our pretraining implements a form of structure learning [52, 53], i.e. learning of the structure (concepts) underlying a family of tasks, which in general facilitates subsequent learning of new representatives. In our networks it enables learning of representatives without synaptic modification. Experiments indicate that animals and humans employ structure learning for example for motor tasks, which requires presentation of a variety of representative tasks and involves a reduction of the dimensionality of the search space, as in our model [52, 53]. Evolution or network plasticity should implement structure learning in biology. Since their functioning is largely unknown, we employ a simple reservoir computing scheme and comparably small neural networks. Only the readout weights, a small fraction of the network weights, are trained. Our dynamically learned tasks have similar difficulty as those used to introduce FORCE weight learning [6]. They are low-dimensional; this may often be the relevant case for biological neural networks, e.g., when learning movements [54].

In experimental physics and engineering, our scheme may find application in neuromorphic computing. Here, intrinsically plastic weights are costly and often difficult to realize, while outsourcing the learning to external controllers introduces computational bottlenecks [55]. As an example, in analog, photonic neuromorphic computing, network weights are externally set to generate desired output dynamics [56–58]. Our scheme may allow such systems to intrinsically learn and thereby fully reap their speed benefits. For spiking hardware, our networks may be efficiently translated into spiking ones [59]. Dynamical learning may reduce the size and power consumption of such hardware, for example in autonomous robots [60].

Our approach suggests a new method for the prediction of chaotic systems [61, 62], which searches for similarity within a predefined family of dynamics and leaves the networks structurally invariant and flexible.

A possible example for dynamical learning in biology is the quick learning of new movements [53, 63],

perhaps with subsequent consolidation by plasticity. Another example may be short-term memory of single items and temporal sequences [64, 65]. Our theory predicts that even complicated dynamics may be memorized in biological neural networks without synaptic modification.

-
- [1] D. V. Buonomano and M. M. Merzenich, *Science* **267**, 1028 (1995).
 - [2] P. F. Dominey, *Biol. Cybern.* **73**, 265 (1995).
 - [3] H. Jaeger and H. Haas, *Science* **304**, 78 (2004).
 - [4] W. Maass, T. Natschläger, and H. Markram, *Neural Comput.* **14**, 2531 (2002).
 - [5] M. B. Westover, C. Eliasmith, and C. H. Anderson, *Neurocomputing* **44-46**, 691 (2002).
 - [6] D. Sussillo and L. F. Abbott, *Neuron* **63**, 544 (2009).
 - [7] M. Lukosevicius, H. Jaeger, and B. Schrauwen, *Künstl. Intell.* **26**, 365 (2012).
 - [8] M. Y. Ismail and J. C. Principe, in *Proc. Systems and Computers Conf. Record of The Thirtieth Asilomar Conf. Signals* (1996) pp. 1083–1087 vol.2.
 - [9] T. Miconi, *eLife* **6**, e20899 (2017).
 - [10] B. DePasquale, C. J. Cueva, K. Rajan, G. S. Escola, and L. F. Abbott, *PLoS One* **13**, e0191527 (2018).
 - [11] <https://github.com/chklos/dynamical-learning>.
 - [12] O. Schütze, X. Esquivel, A. Lara, and C. A. C. Coello, *IEEE Trans. Evolutionary Computation* **16**, 504 (2012).
 - [13] H. Jaeger, arXiv:1403.3369 (2014).
 - [14] H. Jaeger, *Journal of Machine Learning Research* **18**, 1 (2017).
 - [15] A. Dembo and T. Kailath, *IEEE Transactions on Neural Networks* **1**, 58 (1990).
 - [16] M. Jabri and B. Flower, *IEEE Transactions on Neural Networks* **3**, 154 (1992).
 - [17] G. Cauwenberghs, in *Advances in Neural Information Processing Systems*, Vol. 5 (1993) pp. 244–251.
 - [18] H. S. Seung, *Neuron* **40**, 1063 (2003).
 - [19] C. Beer and O. Barak, arXiv:1805.09603 (2018).
 - [20] D. P. Kingma and J. Ba, in *Proceedings of the 3rd International Conference on Learning Representations*, Vol. 3 (2015).
 - [21] R. L. Redondo and R. G. M. Morris, *Nat. Rev. Neurosci.* **12**, 17 (2011).
 - [22] Z. Yu, D. Kappel, R. Legenstein, S. Song, F. Chen, and W. Maass, arXiv:1606.00157 (2016).
 - [23] W. C. Abraham, *Nat. Rev. Neurosci.* **9**, 387 (2008).
 - [24] L. A. Feldkamp, G. V. Puskorius, and P. C. Moore, in *Proceedings of International Conference on Neural Networks (ICNN'96)*, Vol. 1 (1996) pp. 155–160 vol.1.
 - [25] L. A. Feldkamp, G. V. Puskorius, and P. C. Moore, *Information Sciences* **98**, 217 (1997).
 - [26] A. S. Younger, P. R. Conwell, and N. E. Cotter, *IEEE Transactions on Neural Networks* **10**, 272 (1999).
 - [27] S. Hochreiter, A. S. Younger, and P. R. Conwell, in *Artificial Neural Networks — ICANN 2001*, Lecture Notes in Computer Science, edited by G. Dorffner, H. Bischof, and K. Hornik (Springer Berlin Heidelberg, 2001) pp. 87–94.

- [28] A. S. Younger, S. Hochreiter, and P. R. Conwell, in *IJCNN'01. International Joint Conference on Neural Networks. Proceedings (Cat. No.01CH37222)* (2001) pp. 2001–2006 vol.3.
- [29] R. A. Santiago, in *2004 IEEE International Joint Conference on Neural Networks (IEEE Cat. No.04CH37541)*, Vol. 1 (2004) pp. 189–194.
- [30] A. Santoro, S. Bartunov, M. Botvinick, D. Wierstra, and T. Lillicrap, in *International Conference on Machine Learning* (2016) pp. 1842–1850.
- [31] G. Bellec, D. Salaj, A. Subramoney, R. Legenstein, and W. Maass, arXiv:1803.09574 (2018).
- [32] G. V. Puskorius and L. A. Feldkamp, *IEEE Trans. Neural Netw.* **5**, 279 (1994).
- [33] L. A. Feldkamp and G. V. Puskorius, in *Proceedings of 1994 IEEE International Conference on Neural Networks (ICNN'94)*, Vol. 4 (IEEE, Orlando, FL, USA, 1994) pp. 2377–2382.
- [34] L. A. Feldkamp and G. V. Puskorius, in *Proceedings of International Conference on Neural Networks (ICNN'97)* (1997) pp. 773–778 vol.2.
- [35] M. Oubbati and G. Palm, *Neural Computing and Applications* **19**, 103 (2010).
- [36] F. wyffels, J. Li, T. Waegeman, B. Schrauwen, and H. Jaeger, *Biol. Cybern.* **108**, 145 (2014).
- [37] H. Jaeger and D. Eck, in *Modeling Communication with Robots and Virtual Humans* (Springer, Berlin, Heidelberg, 2008) pp. 310–335.
- [38] M. Oubbati, P. Levi, and M. Schanz, in *Proceedings of the 2005 IEEE International Symposium on, Mediterrean Conference on Control and Automation Intelligent Control, 2005.* (2005) pp. 473–478.
- [39] L. A. Feldkamp and G. V. Puskorius, in *Proceedings of 1994 33rd IEEE Conference on Decision and Control* (1994) pp. 2754–2759 vol.3.
- [40] L. A. Feldkamp, D. V. Prokhorov, and T. M. Feldkamp, *Neural Networks* **16**, 683 (2003).
- [41] E. D. Sontag, in *Proc. Seventh Yale Workshop on Adaptive and Learning Systems* (1992) pp. 73–79.
- [42] K.-I. Funahashi and Y. Nakamura, *Neural Networks* **6**, 801 (1993).
- [43] K.-K. K. Kim, E. R. Patrón, and R. D. Braatz, *Neural Networks* **98**, 251 (2018).
- [44] N. E. Cotter and P. R. Conwell, in *1990 IJCNN International Joint Conference on Neural Networks* (1990) pp. 553–559 vol.3.
- [45] N. E. Cotter and P. R. Conwell, in *IJCNN-91-Seattle International Joint Conference on Neural Networks* (1991) pp. 799–801 vol.1.
- [46] S. Lim and M. S. Goldman, *Nat. Neurosci.* **16**, 1306 (2013).
- [47] W. Maass, P. Joshi, and E. D. Sontag, *PLOS Comput. Biol.* **3**, e165 (2007).
- [48] D. Sussillo and O. Barak, *Neural Comput.* **25**, 626 (2013).
- [49] R. Pascanu and H. Jaeger, *Neural Networks* **24**, 199 (2011).
- [50] V. Mante, D. Sussillo, K. V. Shenoy, and W. T. Newsome, *Nature* **503**, 78 (2013).
- [51] K. J. Boström, H. Wagner, M. Prieske, and M. de Lussanet, *Human Movement Science* **32**, 880 (2013).
- [52] B. J. Lansdell and K. P. Kording, arXiv:1811.00231 (2018).
- [53] D. A. Braun, C. Mehring, and D. M. Wolpert, *Behavioural Brain Research* **206**, 157 (2010).
- [54] J. A. Gallego, M. G. Perich, L. E. Miller, and S. A. Solla, *Neuron* **94**, 978 (2017).
- [55] E. Chicca, F. Stefanini, C. Bartolozzi, and G. Indiveri, *Proc. IEEE* **102**, 1367 (2014).

- [56] F. Duport, A. Smerieri, A. Akrouf, M. Haelterman, and S. Massar, *Sci. Rep.* **6** (2016).
- [57] A. N. Tait, T. F. de Lima, E. Zhou, A. X. Wu, M. A. Nahmias, B. J. Shastri, and P. R. Prucnal, *Sci. Rep.* **7** (2017).
- [58] P. Antonik, M. Haelterman, and S. Massar, *Phys. Rev. Appl.* **7** (2017).
- [59] D. Thalmeier, M. Uhlmann, H. J. Kappen, and R.-M. Memmesheimer, *PLoS Comput. Biol.* **12**, e1004895 (2016).
- [60] C. D. Schuman, T. E. Potok, R. M. Patton, J. D. Birdwell, M. E. Dean, G. S. Rose, and J. S. Plank, *arXiv:1705.06963* (2017).
- [61] J. Pathak, B. Hunt, M. Girvan, Z. Lu, and E. Ott, *Phys. Rev. Lett.* **120**, 024102 (2018).
- [62] R. S. Zimmermann and U. Parlitz, *Chaos* **28**, 043118 (2018).
- [63] M. G. Perich, J. A. Gallego, and L. E. Miller, *Neuron* **100**, 964 (2018).
- [64] K. K. Sreenivasan and M. D'Esposito, *Nat. Rev. Neurosci.* **20**, 466 (2019).
- [65] K. Oberauer, *Trends Cogn. Sci.* **23**, 798 (2019).